SAND2016-8132PE

Exceptional service in the national interest

Sandia National Laboratories

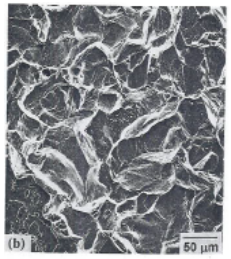

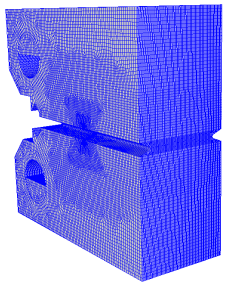
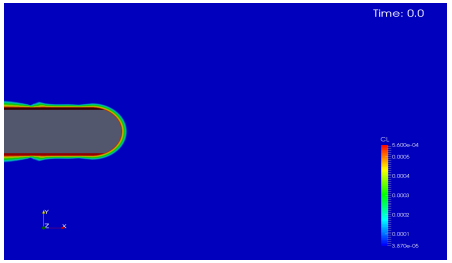

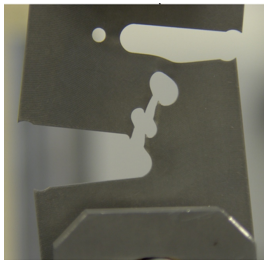
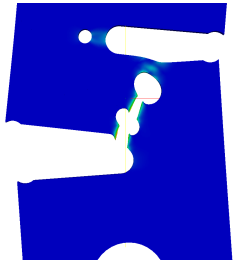
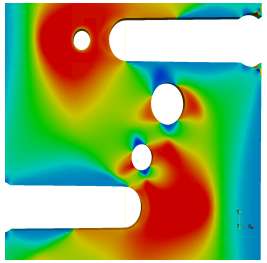
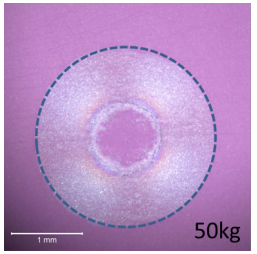

Fracture Mechanics R&D at Sandia National Laboratories

Jonathan A. Zimmerman
Manager – Hydrogen and Materials Science Department

Key Contributors: Edmundo Corona, James W. Foulk III, Reese Jones, E. David Reedy Jr., Joseph Ronevich

U.S. DEPARTMENT OF ENERGY

NNSA National Nuclear Security Administration

Sandia National Laboratories is a multi-program laboratory managed and operated by Sandia Corporation, a wholly owned subsidiary of Lockheed Martin Corporation, for the U.S. Department of Energy's National Nuclear Security Administration under contract DE-AC04-94AL85000. SAND NO. 2011-XXXXP

Predicting fracture – a formidable challenge!

- Sandia's success at its national security missions rely upon:
  - Understanding the mechanical behavior of materials used within its engineering applications
  - Qualification of those materials and achieving a desired reliability of the resultant technology
  - High-fidelity models and high-performance computing platforms that enable prediction of both material behavior and performance of engineering components
- Some areas of investigation permeate multiple missions. For example, understanding how hydrogen affects the structural integrity and mechanical performance of stainless steels is relevant to both nuclear weapon stockpile stewardship and sustainable alternative energies for transportation.
- **Our focus**: develop fundamental understanding and predictive capabilities for crack nucleation, initiation and propagation (as well as ductile deformation) in materials relevant to Sandia's technological systems.

Recent efforts at Sandia

- Fatigue crack growth in pipeline steels and their welds in high-pressure hydrogen gas
- Simulating hydrogen embrittlement – and hydrogen isotope embrittlement – and fast pathways for diffusion
- Initiation and growth of subcritical cracks in chemically reactive environments, including low-permeability geomaterials
- Calibration of the Johnson-Cook strength and failure models to accurately represent ductile failure under shear-dominated states
- Cohesive zone-based fracture modeling of polymer/solid interfaces
- Sandia's Fracture Challenges – predicting crack initiation and propagation around the nation and around the world

Fatigue crack growth in pipeline steels and their welds in high-pressure hydrogen gas

Sandia National Laboratories

- Hydrogen embrittlement is recognized as a potential reliability issue for steel pipelines (1,500 miles of steel hydrogen pipelines already in use in the U.S.)

X52 or X65 Line Pipe (i.e. base metal)

Microstructure of base metal affects crack growth rates

Welds may be more susceptible to embrittlement

Welding to join or repair pipe

Images used with permission from U.S Pipeline, and Canadian Energy Pipeline Association

Daily pressure fluctuations can result in fatigue loading which can affect embrittlement

Key Questions:

1. How does H_2 act to embrittle the metal during fatigue (fluctuating) loading?
2. Do all microstructures (base, weld, HAZ) act the same?
3. Can gas impurities mitigate embrittlement effect?

Approach: Measure fatigue crack growth

- Measure fatigue crack growth in steels in high-pressure H_2 gas (Hydrogen Effects on Materials Laboratory)
  - Industrially relevant pipeline grades
  - Representative service environment
  - Fatigue crack growth data will be the basis for requirements of the ASME B31.12 code "Hydrogen Piping and Pipelines"

- Assess variables that influence hydrogen embrittlement in pipeline steels
  - Microstructure: Base metal vs Welds vs Heat Affected Zones
  - Gas impurities

X65

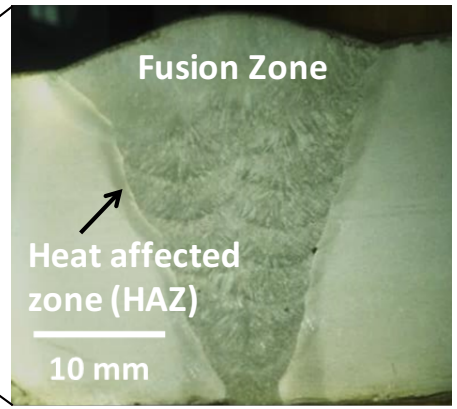

Gas metal arc weld (GMAW)

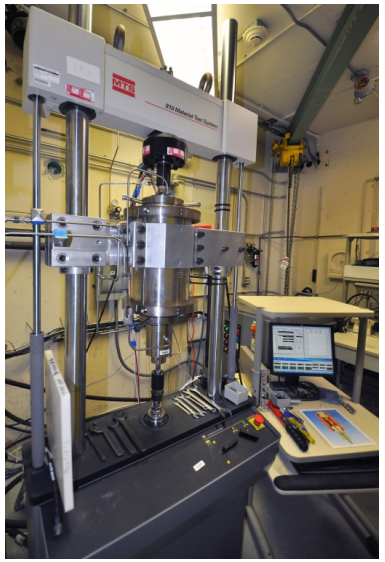

Approach: Correlate microstructure with crack growth

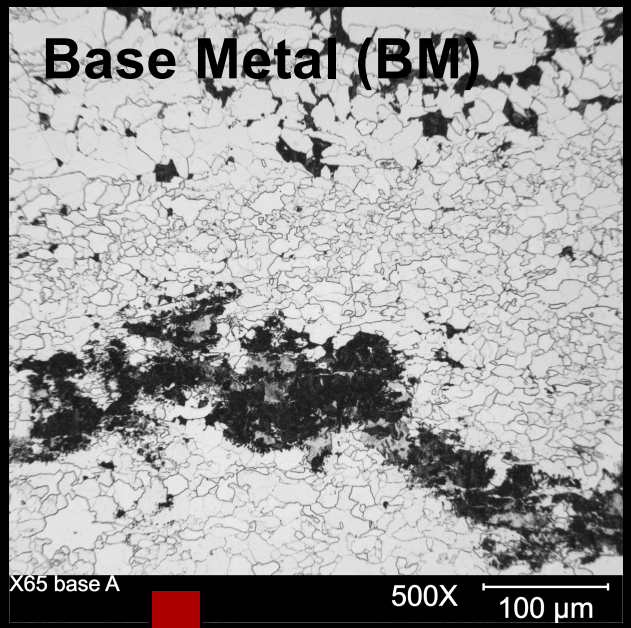

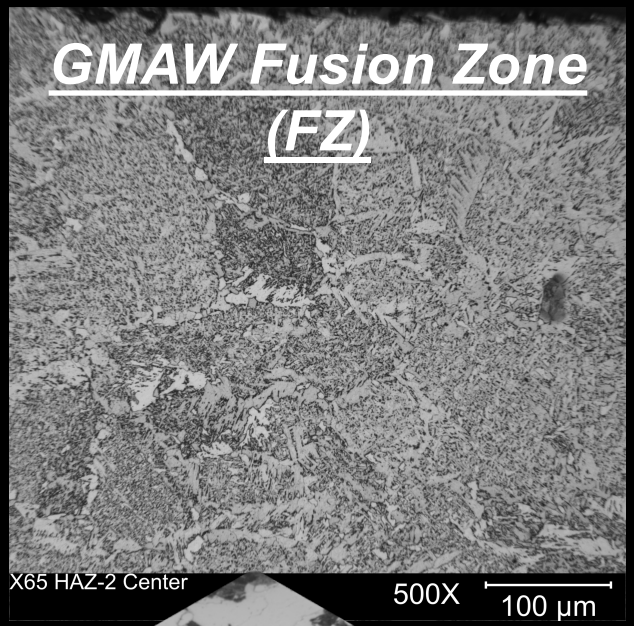

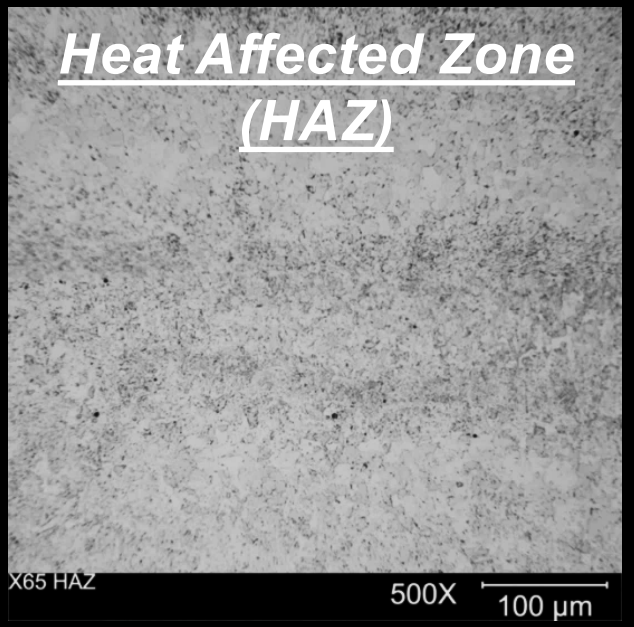

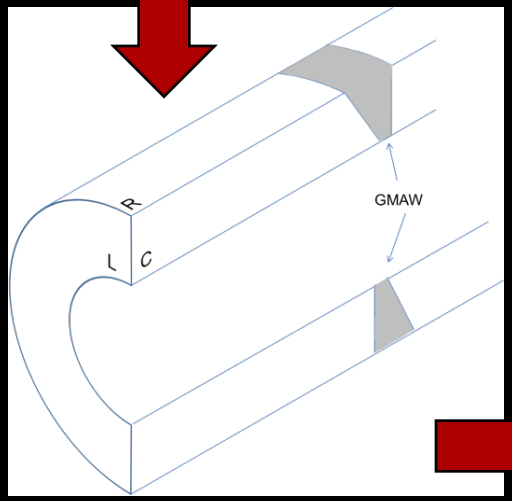

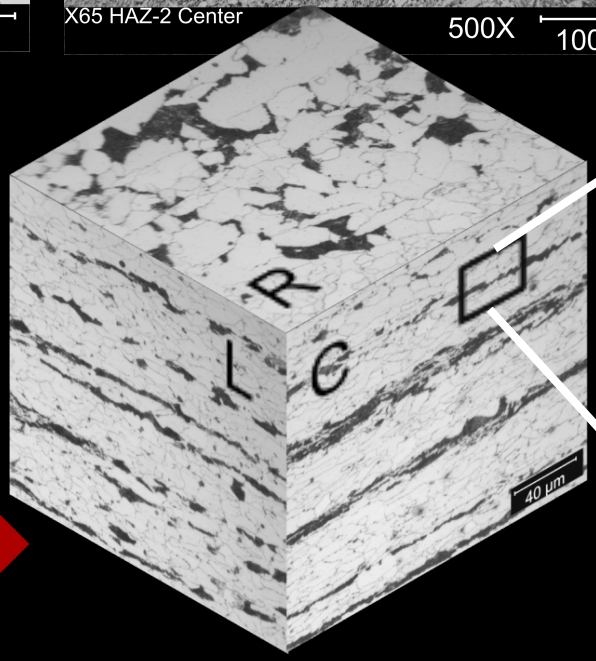

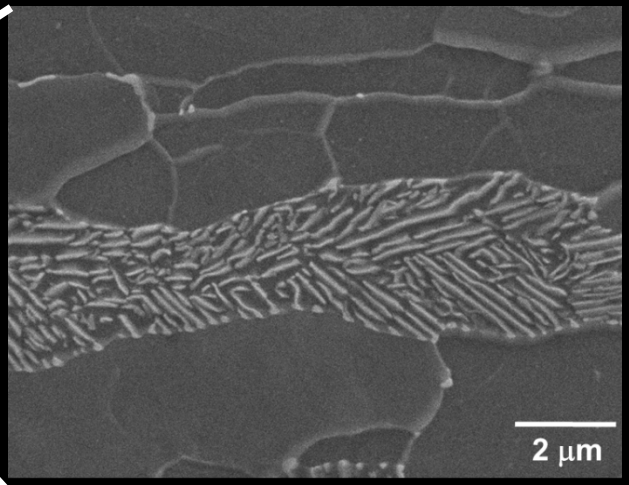

Results: X65 Gas Metal Arc Weld (GMAW)

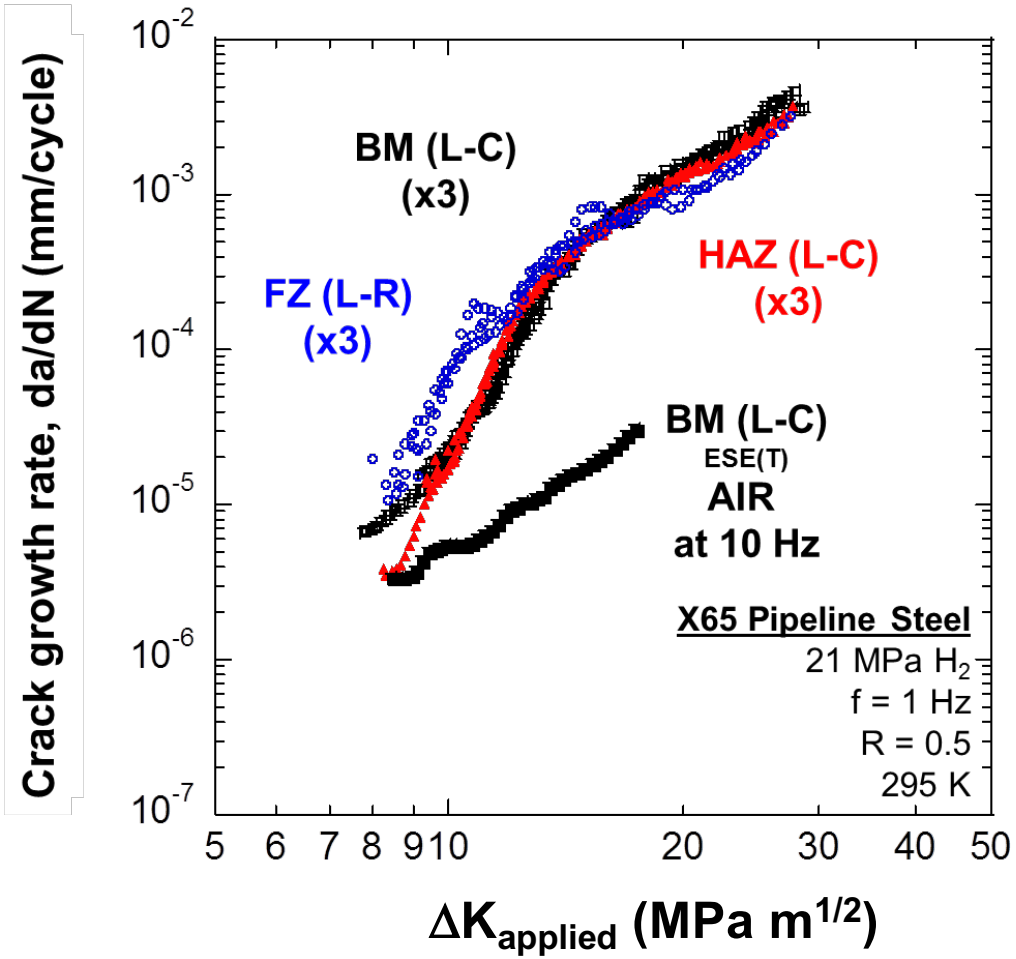

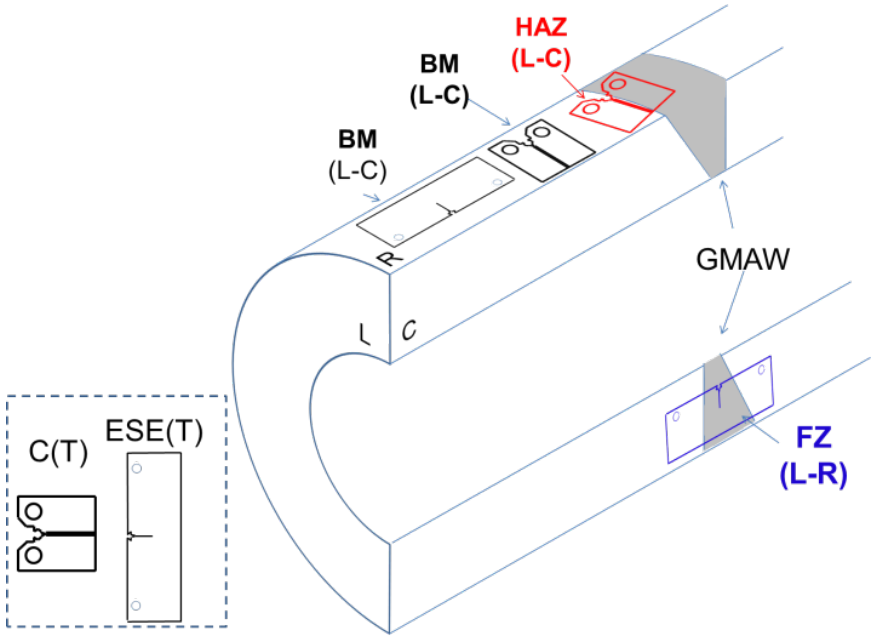

- **Triplicate tests revealed repeatable results**
- **Results did not account for "residual stress" resulting from welding**

J. Ronevich & B. Somerday, *Materials Performance and Characterization*, 2015, submitted.

Must perform analysis to account for contribution of residual stress to driving force, ΔK.

Results: X65 Gas Metal Arc Weld (GMAW)

Sandia National Laboratories

Analysis to account for residual stress in driving force leads to more reliable da/dN vs. ΔK curves.

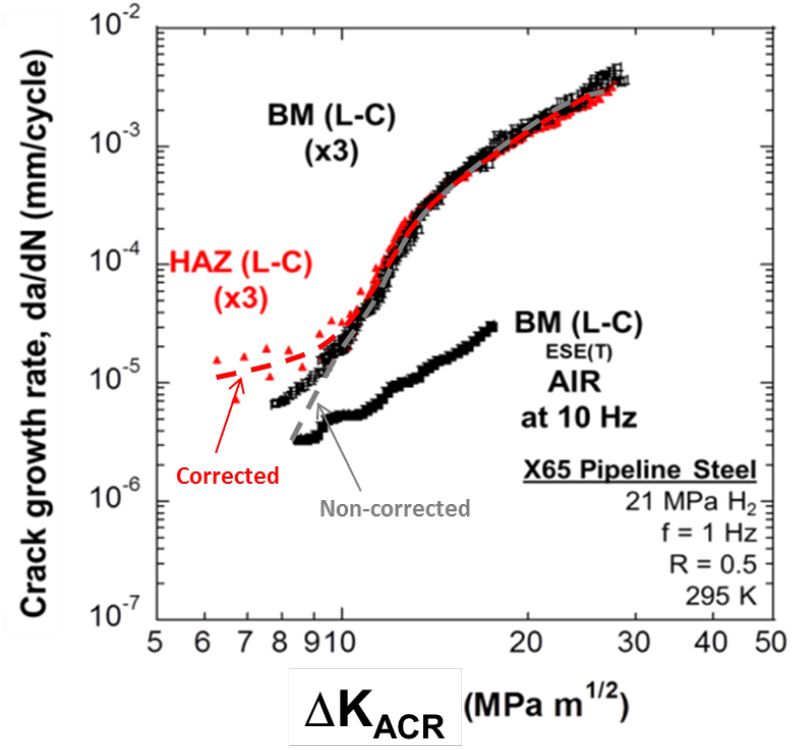

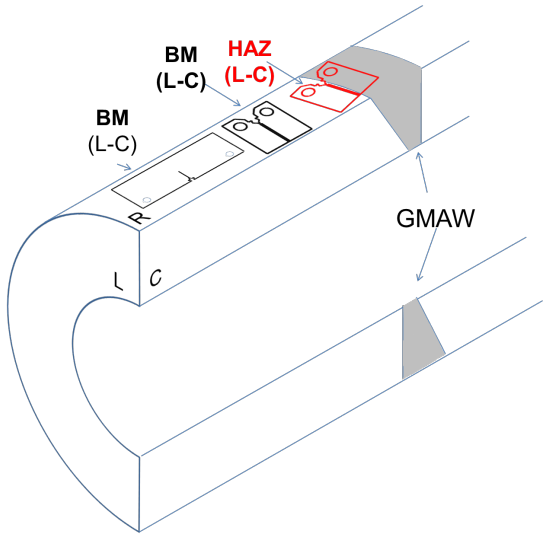

- **Corrections show faster crack growth at lower ΔK than previously determined.**

X65: Crack growth faster in weld heat affected zone than in base metal.

Comparisons of different weld types and steels

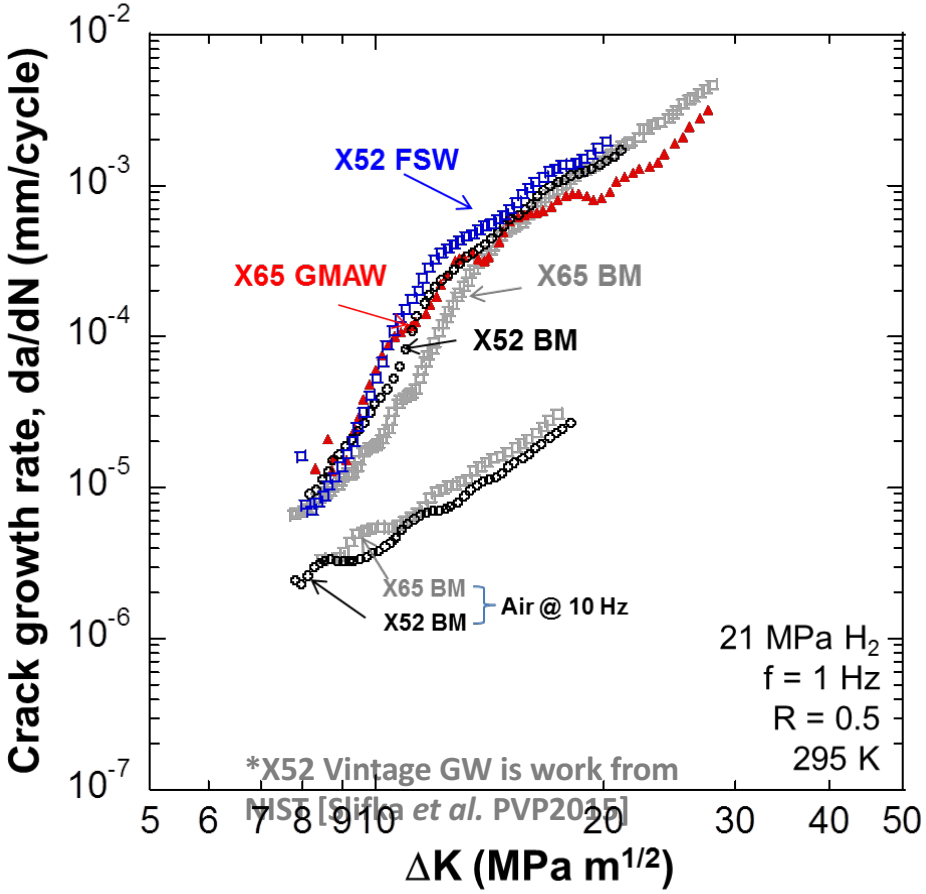

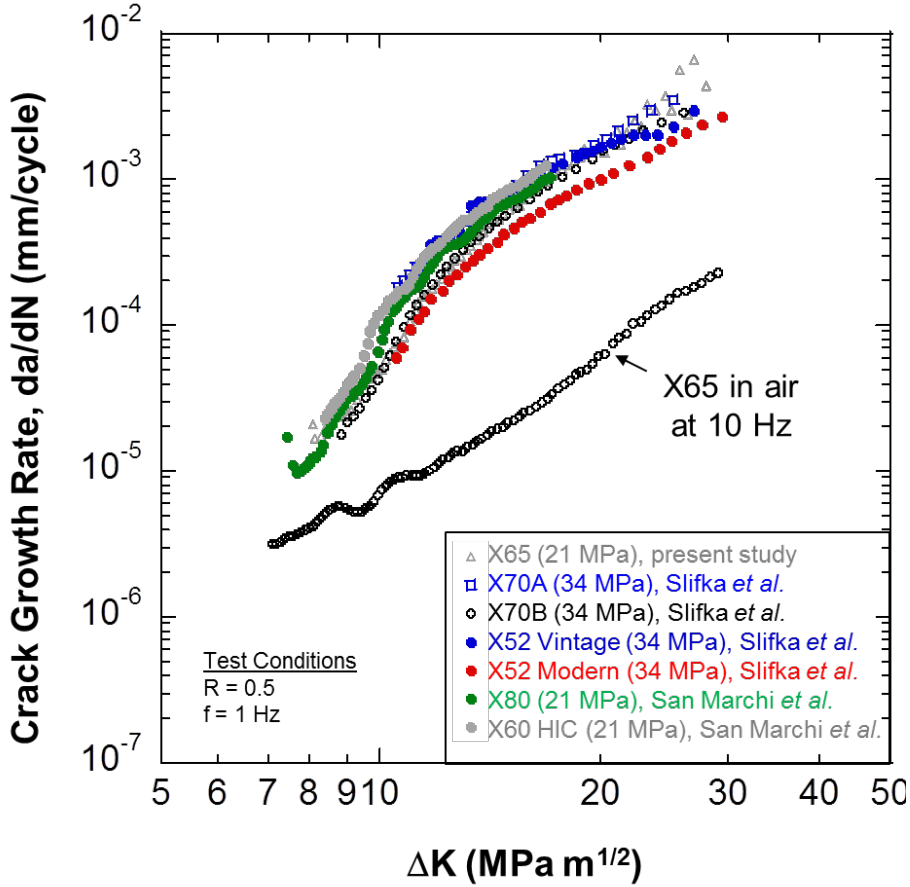

- Friction stir welds and conventional gas metal arc welds exhibit similar crack growth rates in hydrogen.
- Pipelines of different strength exhibit similar hydrogen accelerated fatigue crack growth

Embrittlement Mitigation: Hydrogen uptake retarded by oxygen adsorption on crack-tip surface

Sandia National Laboratories

Potential energy surface scan for H_2 approaching Fe(100) suraface

Staykov et al., *Int J Quantum Chemistry*, 2014

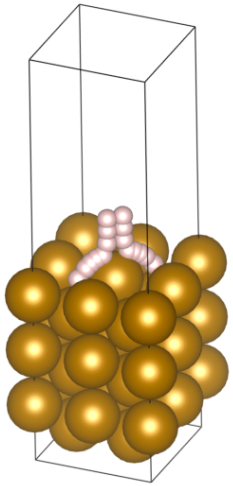

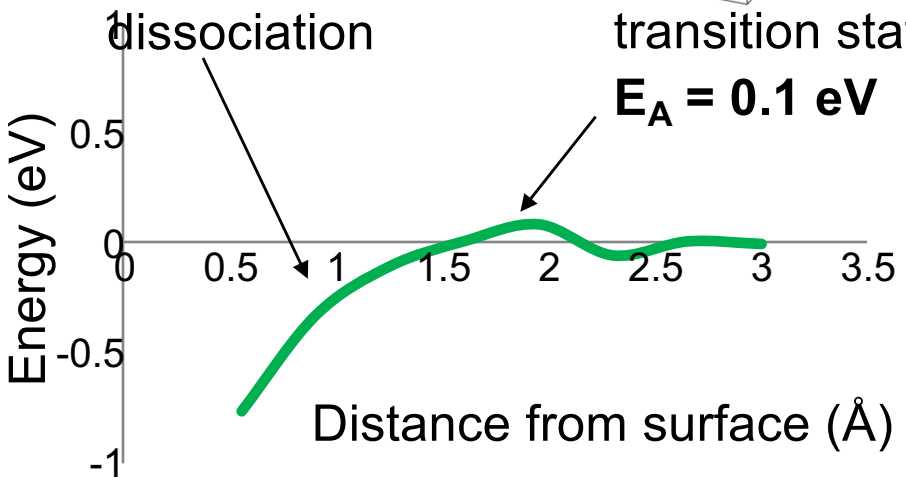

Potential energy surface scan for H_2 approaching Fe(100) surface with preadsorbed O atoms

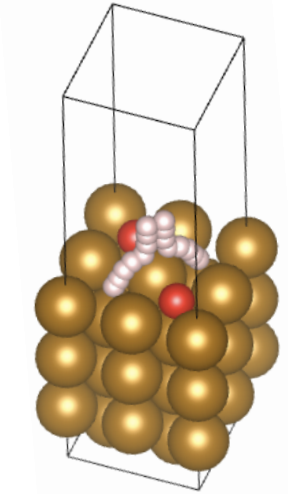

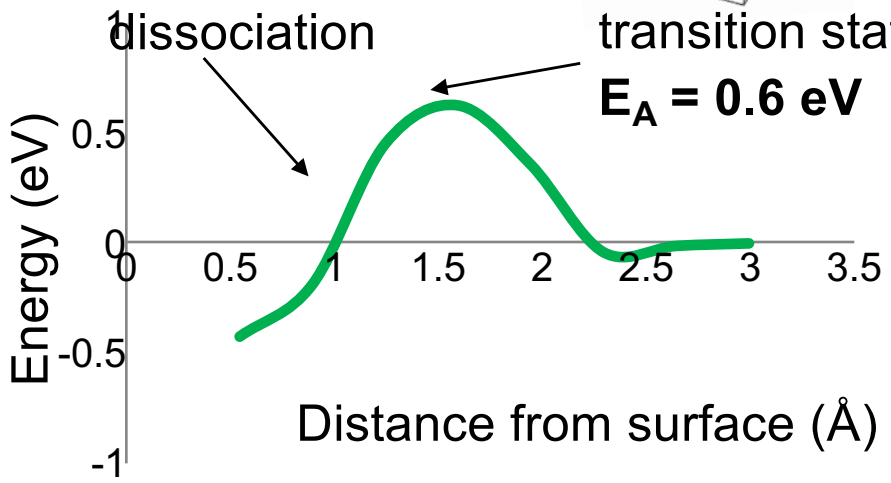

DFT simulations show that pre-adsorbed oxygen inhibits H_2 dissociation.

Embrittlement Mitigation: Testing

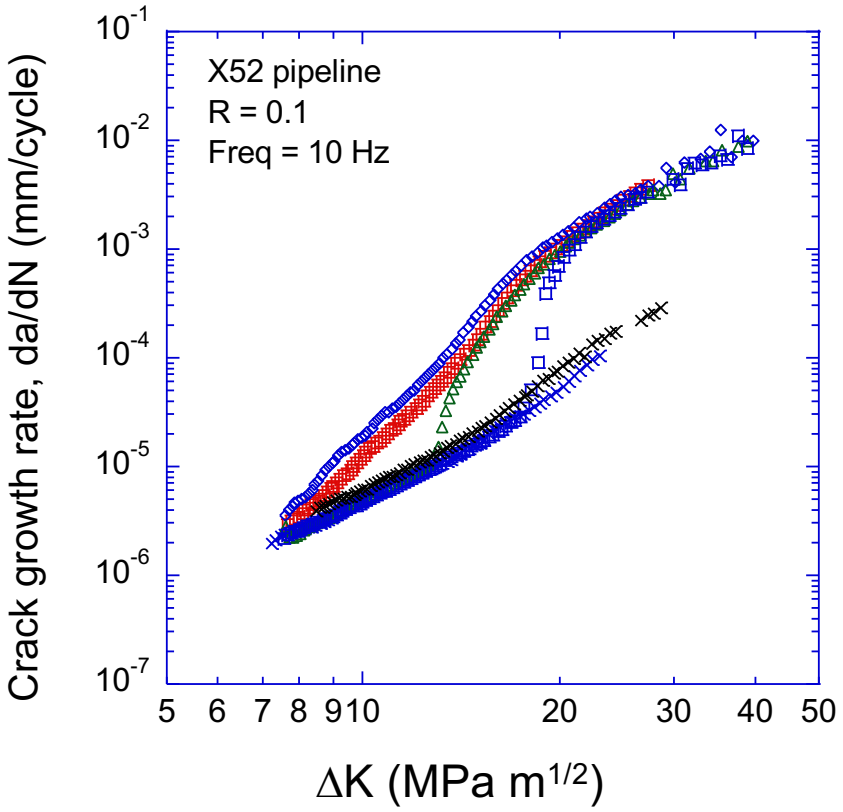

B.P. Somerday et al., *Acta Mater*, 2013

- <0.5 vppm O_2 (R=0.1)
- 10 vppm O_2 (R=0.1)
- 100 vppm O_2 (R=0.1)
- 1000 vppm O_2 (R=0.1)
- 1000 vppm O_2 (R=0.5)
- air

- At lower ΔK, crack growth rates in H_2 environments same as rates in air
- At R=0.1, hydrogen-accelerated crack growth observed at higher ΔK
  - da/dN at onset of hydrogen-accelerated crack growth depends on O_2 concentration
- At R=0.5, hydrogen-accelerated crack growth not observed

Mitigation depends on several variables: O_2 concentration, R-ratio, da/dN, and load cycle frequency.

Embrittlement Mitigation: Modeling H_2 Embrittlement with Oxygen Impurities

Sandia National Laboratories

B. Somerday et al., *Acta Mater* (2013)

Assumptions

- Initial inert-environment crack growth modeled by blunting-resharpening
- Oxygen out-competes hydrogen for adsorption sites on freshly exposed crack-tip surface
- Extent of oxygen adsorption depends on crack-tip area, proportional to crack-growth increment (*da*)
  - when $da < da_{crit}$, crack tip *fully passivated* by oxygen
  - when $da > da_{crit}$, crack tip *not fully passivated* → H uptake
- Model foundation: oxygen delivered to crack tip ($Jh\Delta t$) = oxygen adsorbed on crack tip ($S\theta\pi\Delta a$)
- ***H uptake and accelerated crack growth when*** $f(\Delta a) = f(\Delta a)_{crit} = h(p_{tot}, \Delta K, R, \ldots)$

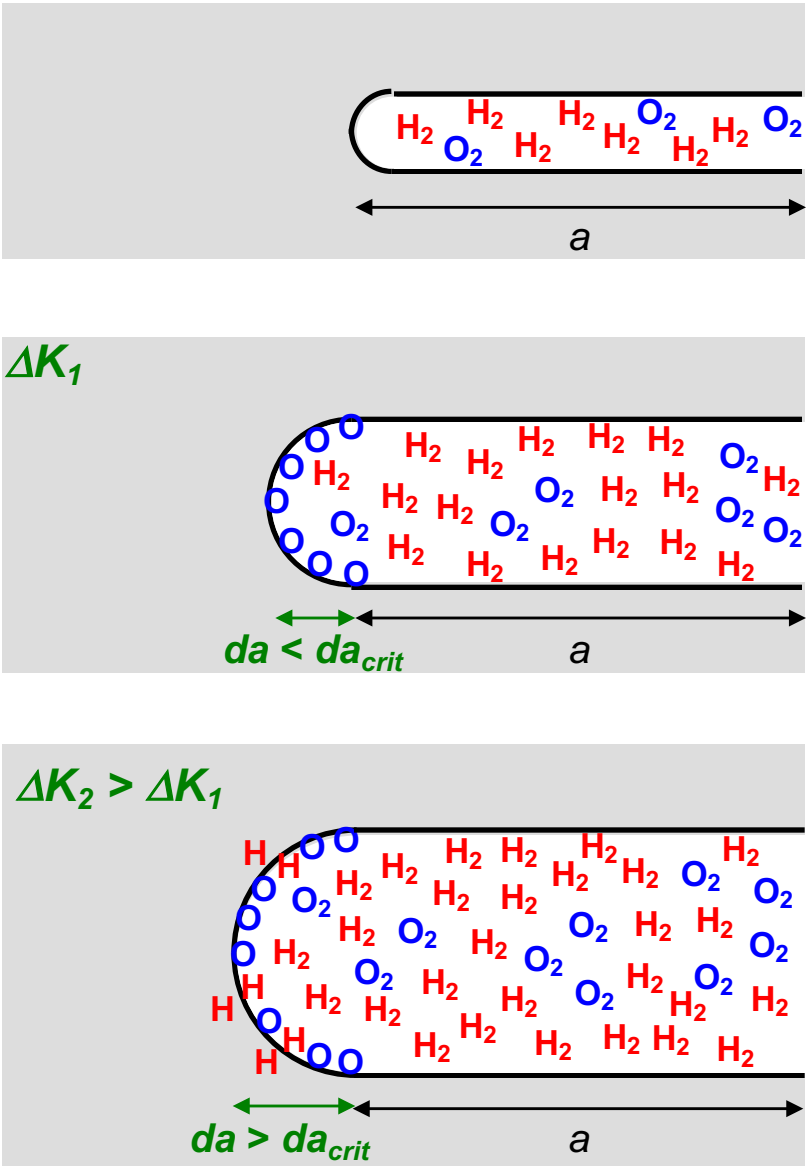

Simulating hydrogen (and hydrogen isotope) embrittlement and fast diffusion

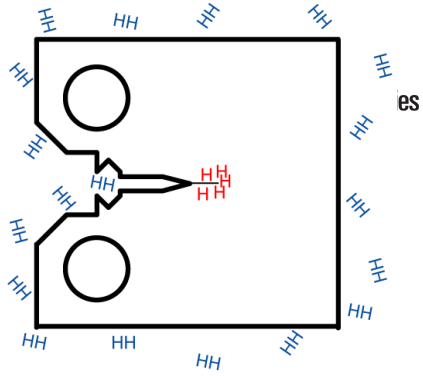

- Motivated through observation
- Strong chemo-mechanical coupling
- Capture sub-grid processes through a surface approach
- Explore fast pathways for diffusion at structural and microstructural scales
- **Develop models for H/T/He embrittlement w/focus on void nucleation**
  - Fracture toughness degrades with increasing helium concentrations
  - Both tritium and helium are requisite for degradation
  - Transition from void evolution to fracture along twin and grain boundaries

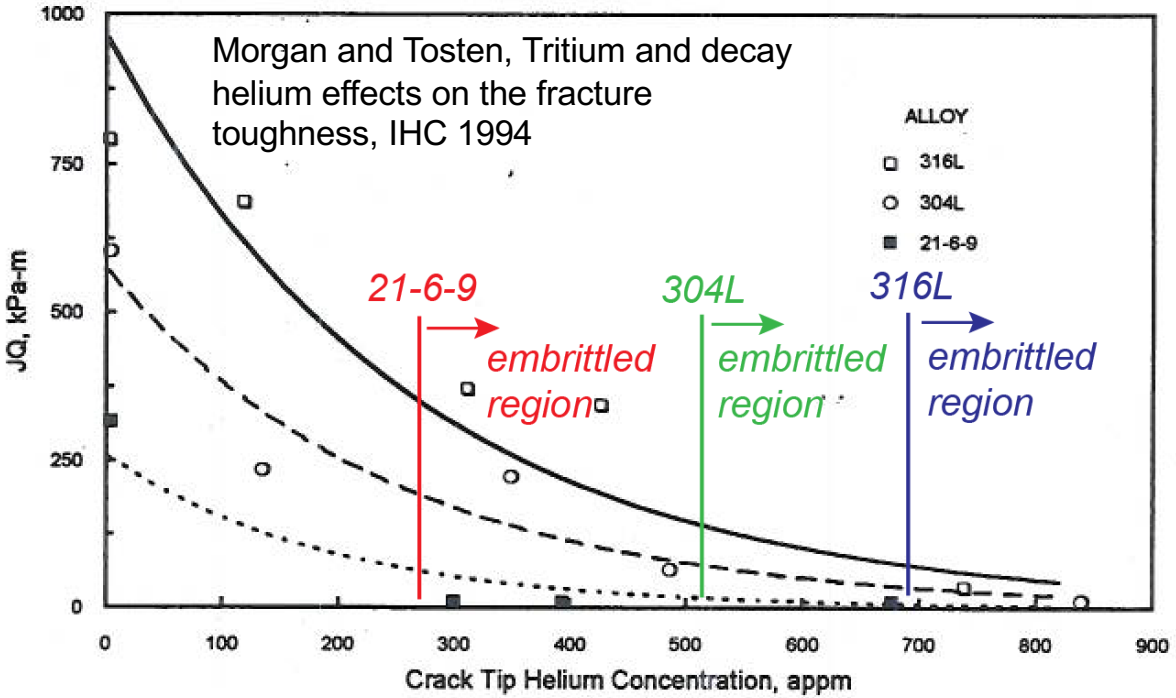

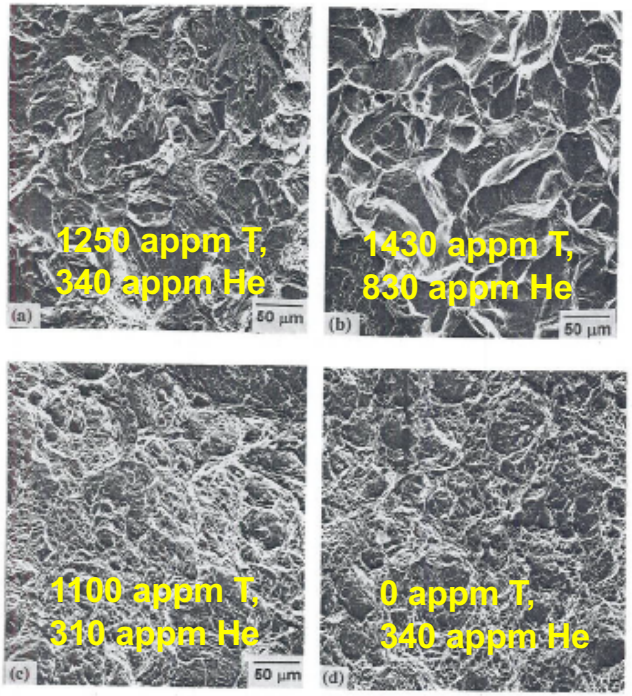

Finite deformation diffusion of hydrogen

Sandia National Laboratories

This path heavily leverages Sofronis/McMeeking (1989)* and Krom (1998). Recent work by Leo and Anand (2013).

Transport of hydrogen in the current configuration

$$D^*\dot{c}_l + C^*\mathrm{div}\boldsymbol{v} - \nabla_{\boldsymbol{x}}\cdot\boldsymbol{d}_l\nabla_{\boldsymbol{x}}c_l - \nabla_{\boldsymbol{x}}\cdot\frac{c_l}{J}\boldsymbol{d}_l\nabla_{\boldsymbol{x}}J + \nabla_{\boldsymbol{x}}\cdot\frac{c_l V_H}{RT}\boldsymbol{d}_l\nabla_{\boldsymbol{x}}\tau_h + \frac{\theta_l}{J}\frac{\partial N_T}{\partial\epsilon_p}\dot{\epsilon}_p - \frac{\theta_t N_T}{J^2}\dot{J} = 0$$

Transport of hydrogen in the reference configuration (push back)

$$D^*\dot{C}_L - \nabla_{\boldsymbol{X}}\cdot d_l\boldsymbol{C}^{-1}\nabla_{\boldsymbol{X}}C_L + \nabla_{\boldsymbol{X}}\cdot\frac{d_l V_H}{RT}\boldsymbol{C}^{-1}\nabla_{\boldsymbol{X}}\tau_h C_L + \theta_T\frac{dN_T}{d\epsilon_p}\dot{\epsilon}_p$$

transient term

diffusion term

advection term from hydrostatic stress

source term from trapping

Deformation-dependent diffusivity $\boldsymbol{D}_L = \boldsymbol{F}^{-1}\boldsymbol{d}_l\boldsymbol{F}^{-T} = d_l\boldsymbol{C}^{-1}$

Capture sub-grid processes for R(a)

Goal: Capture sub-grid processes through methods that regularize the jump

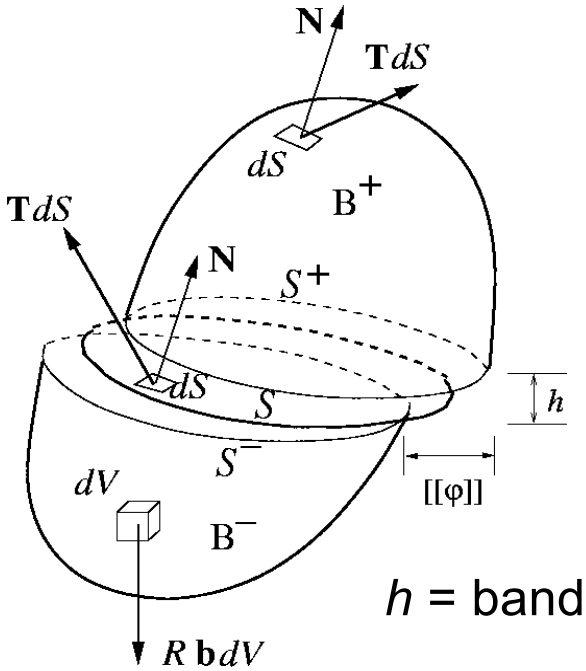

h = band thickness

$$\boldsymbol{F} = \boldsymbol{F}^{\parallel}\boldsymbol{F}^{\perp}$$

$$\boldsymbol{F}^{\parallel} = \boldsymbol{g}_i \otimes \boldsymbol{G}^i$$

$$\boldsymbol{F}^{\perp} = \boldsymbol{I} + \frac{[\![\boldsymbol{\Phi}]\!]}{h} \otimes \boldsymbol{N}$$

$$\boldsymbol{F} = \boldsymbol{F}^{\parallel} + \frac{[\![\boldsymbol{\varphi}]\!]}{h} \otimes \boldsymbol{N}$$

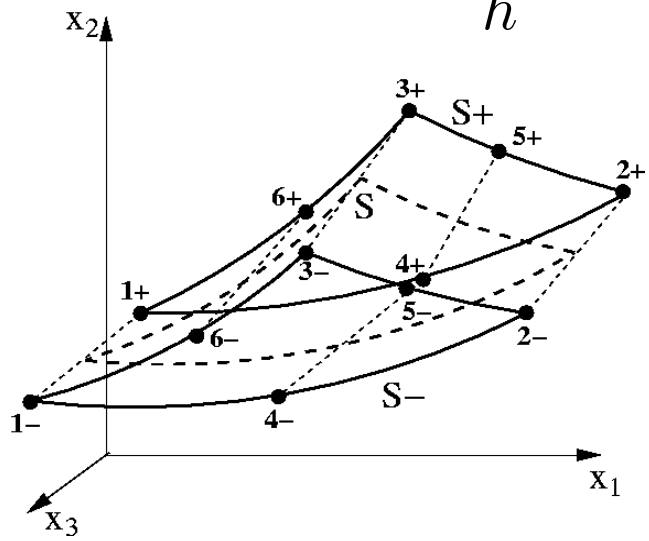

Akin to "cohesive" element

- Finite-deformation kinematics
- Simulation of strain localization
- No additional constitutive assumptions

Yang, Mota and Ortiz (IJNME, 2005), Armero and Garikipati (IJSS, 1996)

Extended sub-grid model for multiphysics

Fox and Simo (1990), Callari, Armero, Abati (2010)

redefine space

$$\boldsymbol{X} = \boldsymbol{\Phi}(\xi^1, \xi^2, \xi^3) = \bar{\boldsymbol{\Phi}}(\xi^1, \xi^2) + \boldsymbol{N}(\xi^1, \xi^2)\xi^3 \qquad \boldsymbol{G}_i = \boldsymbol{\Phi}_{,i} = \frac{\partial \boldsymbol{X}}{\partial \xi^i}$$

include jump in C

$$C(\boldsymbol{X}) = \bar{C}(\bar{\boldsymbol{\Phi}}[\xi^1, \xi^2]) + \frac{[\![C]\!](\bar{\boldsymbol{\Phi}}[\xi^1, \xi^2])}{h}\xi^3 \qquad \nabla_{\boldsymbol{X}} C = (\nabla \boldsymbol{\Phi})^{-T} \frac{\partial C}{\partial \xi^i}$$

Finite element implementation is straightforward

$$\nabla_{\boldsymbol{X}} C\big|_{\xi^3=0} = [B] \begin{bmatrix} \{C\}^+ \\ \{C\}^- \end{bmatrix} = \begin{bmatrix} [B]^+ & [B]^- \end{bmatrix} \begin{bmatrix} \{C\}^+ \\ \{C\}^- \end{bmatrix}$$

$$B^{\pm}_{ia} = \begin{bmatrix} G^1_i & G^2_i & G^3_i \end{bmatrix} \cdot \begin{bmatrix} \frac{1}{2}\frac{\partial N_a}{\partial \xi^1} & \frac{1}{2}\frac{\partial N_a}{\partial \xi^2} & \pm\frac{1}{h}N_a \end{bmatrix}$$

i = # dimensions, *a* = # nodes

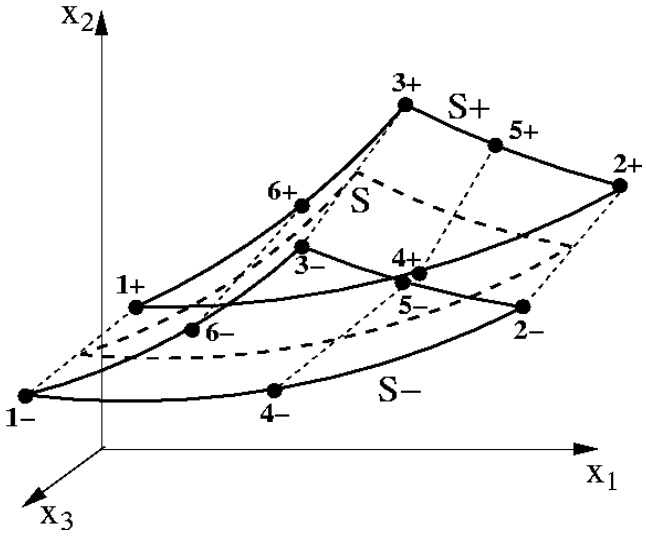

Given this gradient operator, we can use the same PDE for finite-deformation diffusion

$$D^*\dot{C}_L - \nabla_{\boldsymbol{X}} \cdot d_l \boldsymbol{C}^{-1} \nabla_{\boldsymbol{X}} C_L + \nabla_{\boldsymbol{X}} \cdot \frac{d_l V_H}{RT} \boldsymbol{C}^{-1} \nabla_{\boldsymbol{X}} \tau_h C_L + \theta_T \frac{dN_T}{d\epsilon_p} \dot{\epsilon}_p$$

Polycrystal with fast pathway

Grain interface diffusion coupled with mechanical loading:

$$\boldsymbol{D}_L = \boldsymbol{F}^{-1}\boldsymbol{d}_l\boldsymbol{F}^{-T} = d_l\boldsymbol{C}^{-1}$$

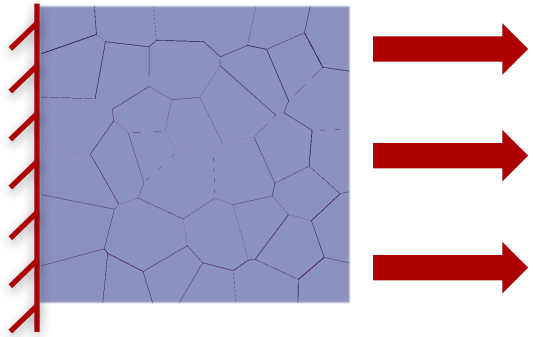

- Stretched in horizontal direction
- Fast pathway = $10^5 D_0$
- Horizontal diffusion
- Vertical diffusion

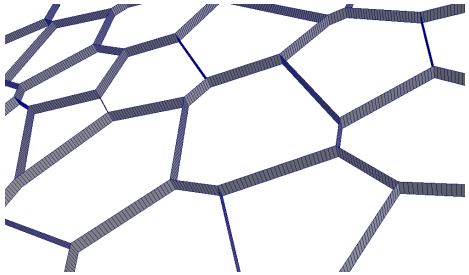

Horizontal diffusion

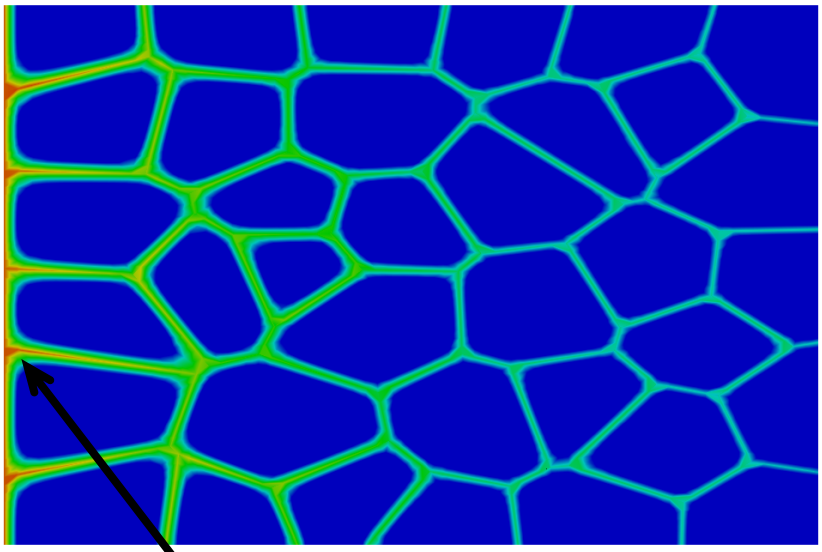

Diffusion slows down due to increasing length.

Vertical diffusion

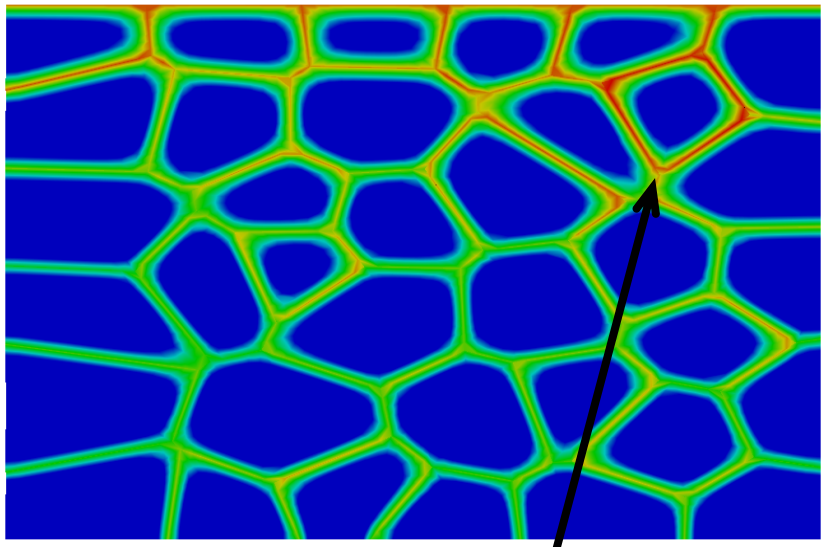

Diffusion speeds up due to decreasing length

Solving 5 fields simultaneously

Units are scaled in the balance of linear momentum, conservation of concentration, and L_2 projection to improve condition number of the system

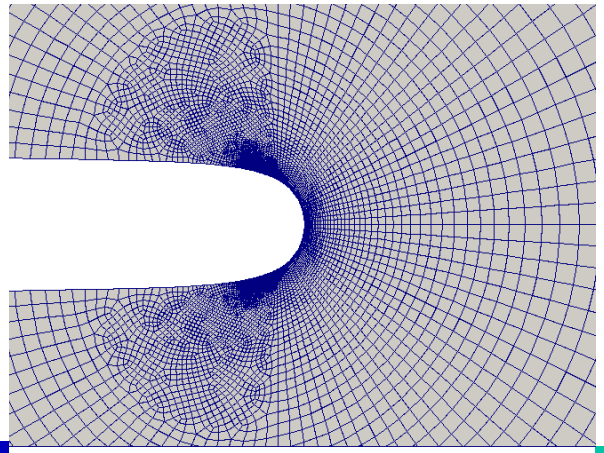

https://software.sandia.gov/albany/

$$D^* \dot{C}_L$$

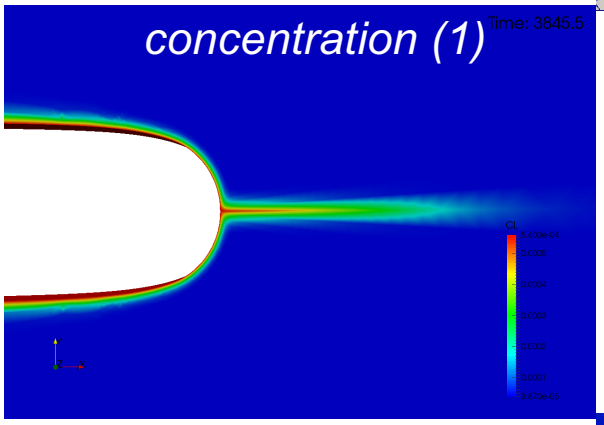

$$\nabla_{\boldsymbol{X}} \cdot d_l \boldsymbol{C}^{-1} \nabla_{\boldsymbol{X}} C_L$$

- Path: $10^5 D_0$
- K_{app}: 85 MPa $m^{1/2}$
- Time: 3850 s

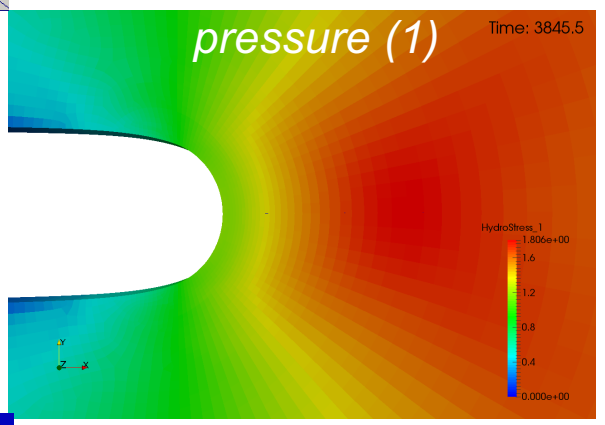

$$\nabla_{\boldsymbol{X}} \cdot \frac{d_l V_H}{RT} \boldsymbol{C}^{-1} \nabla_{\boldsymbol{X}} \tau_h C_L$$

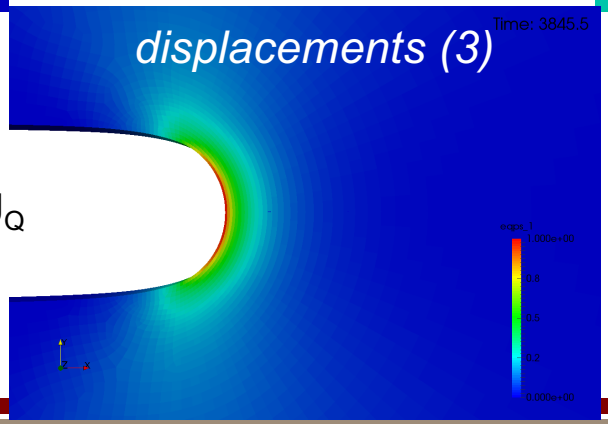

$$\theta_T \frac{dN_T}{d\epsilon_p} \dot{\epsilon}_p$$

NOTE: 85 MPa $m^{1/2}$ is well below J_Q for 21Cr-6Ni-9Mn (220 MPa $m^{1/2}$)

Evolution of lattice hydrogen concentration at crack tip

Sandia National Laboratories

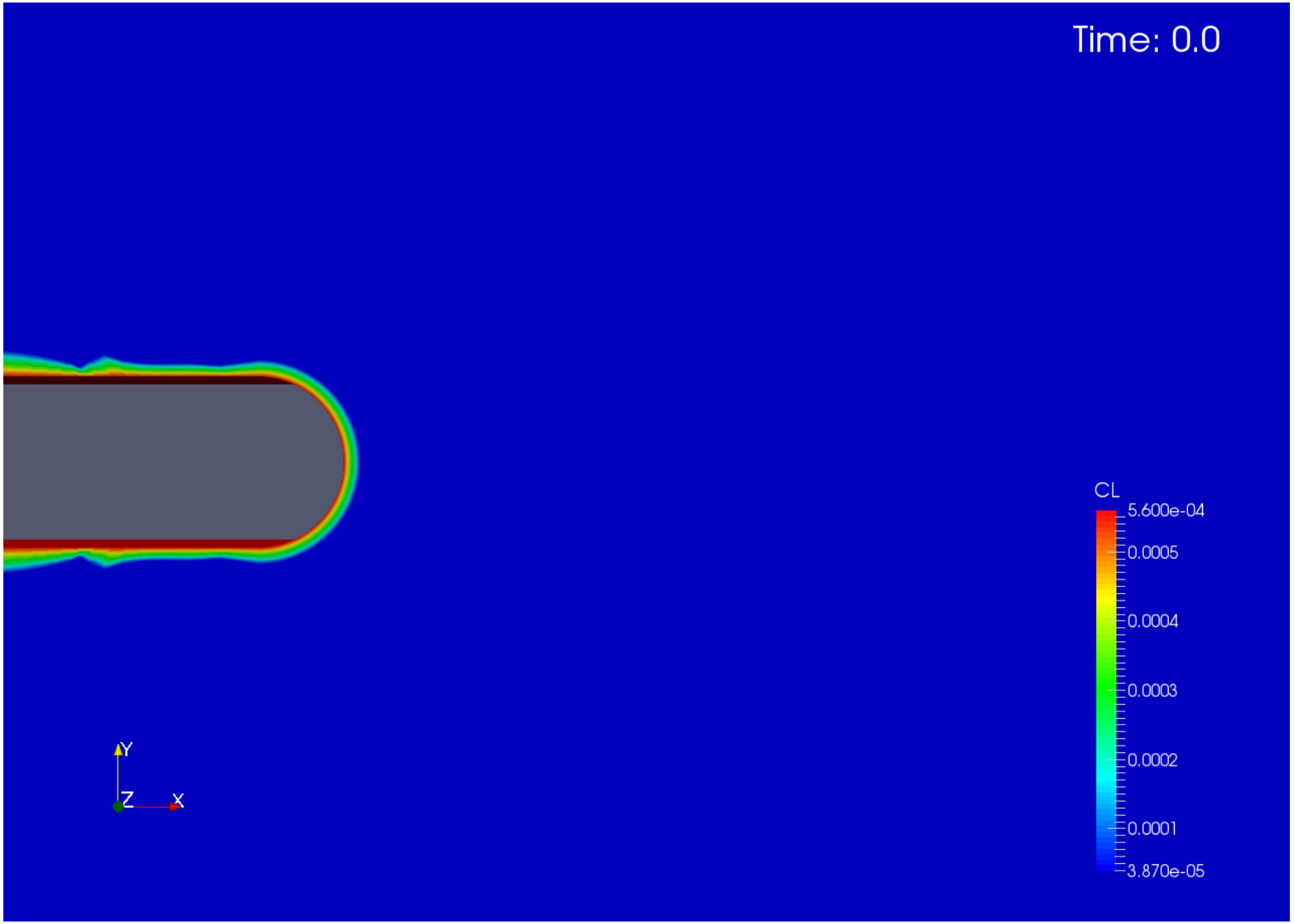

Increasing complexity:
Hydrogen isotope diffusion with helium bubbles

Sandia National Laboratories

We seek to find descriptors of helium bubble formation that result from the radioactive decay of tritium (T) to He.

- Schaldach and Wolfer (2004) focus on the total number of clusters (total bubble density)

1000s of ODEs for helium clusters are condensed into 3 coupled ODEs written in

- Single He (monomers) N_1, total bubble density, N_b, and bubble volume fraction S_b
- ODEs are nonlinear. We can integrate them implicitly with Newton's method
- Chemo-mechanical solution (T, **u**). Solve ODEs (dependent on T) at integration points.

$$\frac{dN_1}{dt} = G(t) - 16\pi(r_1 + r_1)DN_1^2 - 4\pi DN_1\left(\frac{3}{4\pi}\right)^{\frac{1}{3}} S_b^{\frac{1}{3}} N_b^{\frac{2}{3}}$$

$$\frac{dN_b}{dt} = 8\pi(r_1 + r_1)DN_1^2$$

$$\frac{\eta}{\Omega}\frac{dS_b}{dt} = 16\pi(r_1 + r_1)DN_1^2 + 4\pi DN_1\left(\frac{3}{4\pi}\right)^{\frac{1}{3}} S_b^{\frac{1}{3}} N_b^{\frac{2}{3}}$$

$$C_{He} = N_1 + \left(\frac{\eta}{\Omega}\right) S_b$$

G(t) – helium source term
r_1 - initial bubble radius
η - number of He atoms/vacant site
Ω - partial molar volume

Effects of tritium and helium on yield strength

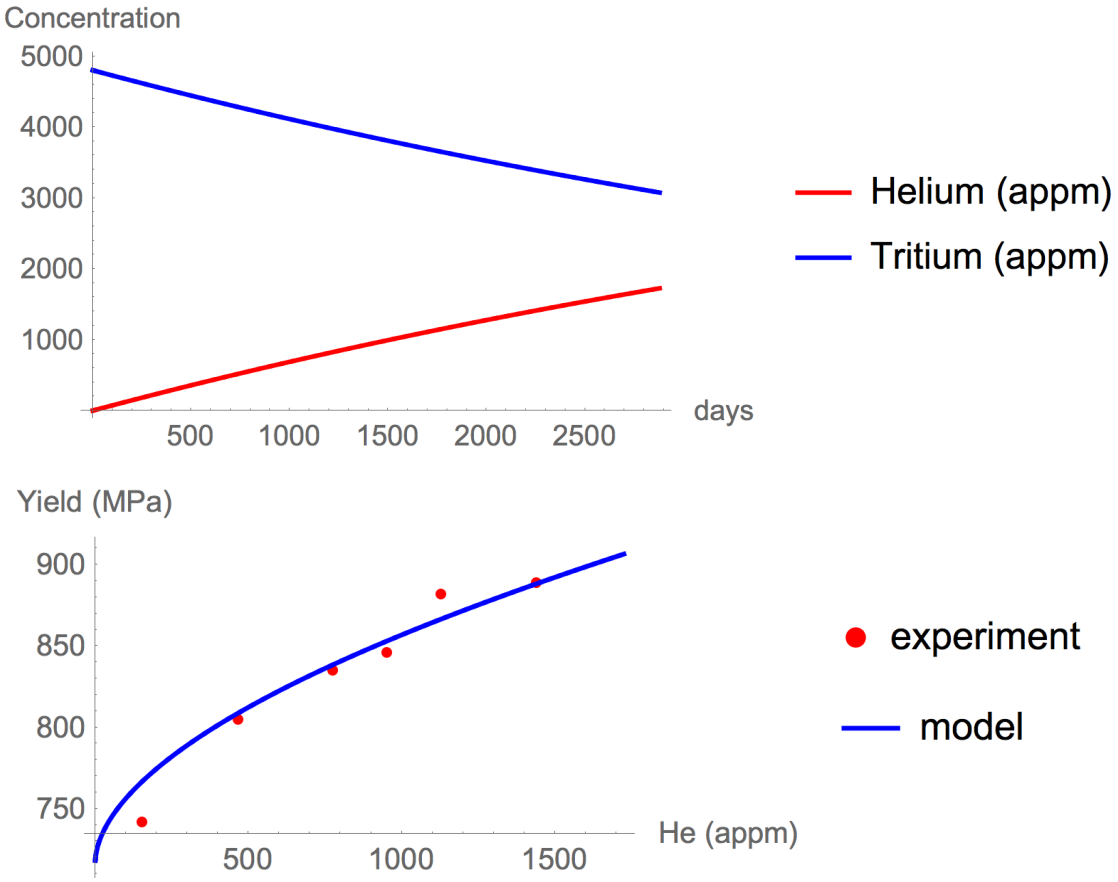

Comparison of current model to experimental data by Robinson and Thomas (1991). Data from hydrogen yields α_1 (hydrogen = tritium). Nonlinearity in fit stems from average bubble radius, not fitting parameter α_2. Both parameters are needed to accurately fit Robinson's data.

From helium bubble ODEs, we have:

N_b total bubble density

S_b bubble volume fraction

Calculate average bubble radius:

$$\bar{R}_b = \left(\frac{3 S_b}{4 \pi N_b} \right)^{\frac{1}{3}}$$

Assumptions for yield stress σ_y:

- Rate independent yield stress σ_0
- Proportional to T concentration, C_T
- Misfit strengthening from He is dominant (Arsenlis, Wolfer, JNM)
- Misfit strengthening varies w/R_b^2
- Normalize w/He atomic radius R_a

$$\sigma_y = \sigma_0 + \alpha_1 C_T + \alpha_2 \left(\frac{\bar{R}_b}{R_a} \right)^2$$

α_1 and α_2 are constants fit to experiments

Change of yield strength is dominant in flow behavior

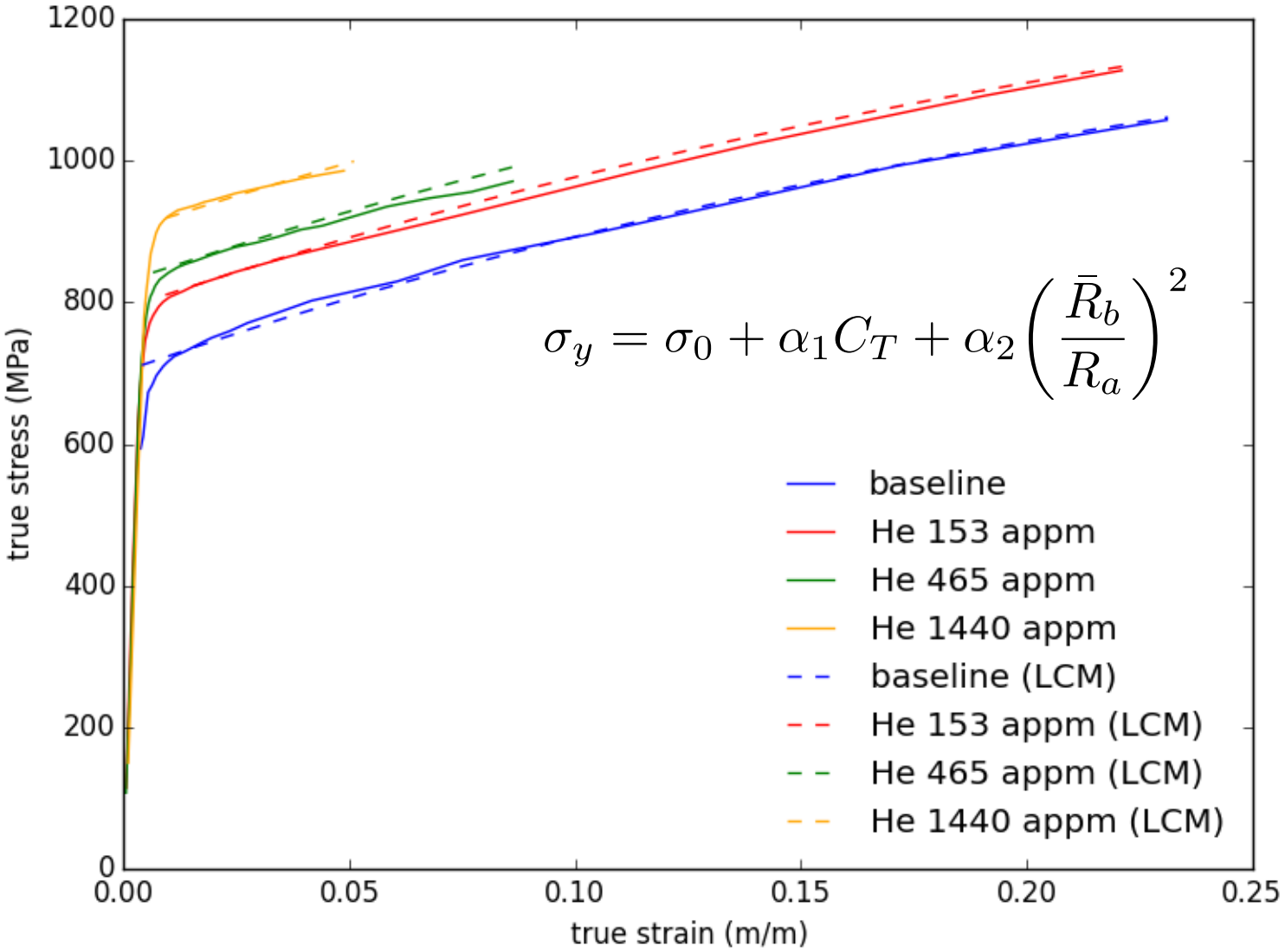

σ_0 = 710 MPa

H = 0.0149μ

R_d = 3.5

α_1 = 63.9 J/mol

α_2 = 4.1 MPa

From Robinson and Thomas, “Accelerated Fracture due to Tritium and Helium in 21-6-9 Stainless Steel” (1991)

T/He nucleation, growth and coalescence

In spirit of Chu and Needleman (1980) we choose an appropriate state variable to capture void nucleation through elevated stresses at pile-ups.

void volume fraction for nucleation — mean ε_{ss} for nucleation

$$f_n(C_T, S_b) = \frac{\phi_{n,0}(S_b)}{\sqrt{2\pi}\sigma_{\epsilon_{ss}}} \exp\left[-\frac{1}{2}\left(\frac{\epsilon_{ss} - \mu_{\epsilon_{ss}}(C_T)}{\sigma_{\epsilon_{ss}}}\right)^2\right]$$

f_n: probability distribution

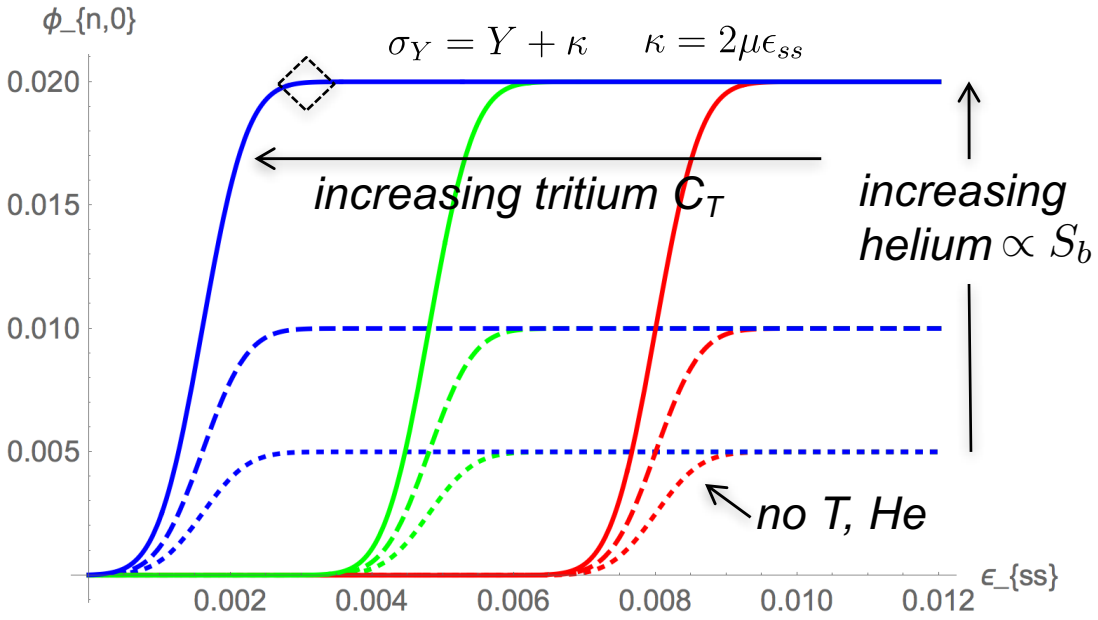

Statistical nucleation: Tritium localizes deformation and enables voids to nucleate earlier in the deformation. Helium-hardened microstructure nucleates more voids.

Initial model for void evolution:

- Void nucleation driven by deformation (dislocations, twins) $\propto \epsilon_{ss}$
  - Tritium C_T hastens process
  - Helium amplifies process
- Void growth through Gurson
- Void coalescence governed by S_b
  - Nucleated voids connected by smaller helium bubbles

A tritium-embrittled, helium-hardened microstructure can move from nucleation to coalescence

Moving forward: develop models to guide discovery, such as dislocation-mediated void nucleation in the presence of hydrogen

Initiation and growth of subcritical cracks in chemically reactive environments (geomaterials)

Sandia National Laboratories

- **Goals**:
  - Develop fundamental understanding of the chemical-mechanical mechanisms that control subcritical cracks in low-permeability geomaterials
  - Link atomic-scale insight to macroscale observables and directly address how chemical environment affects mechanical behavior

fracking

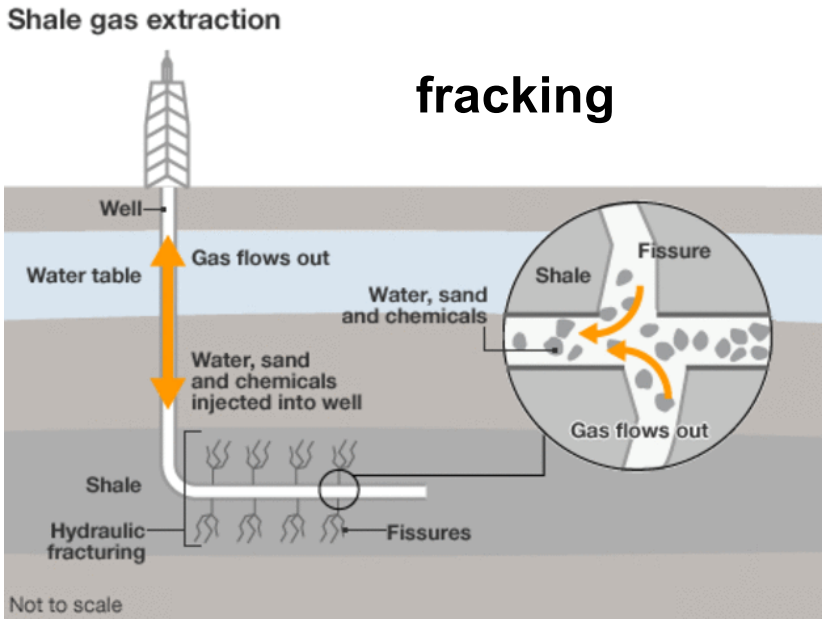

sequestration

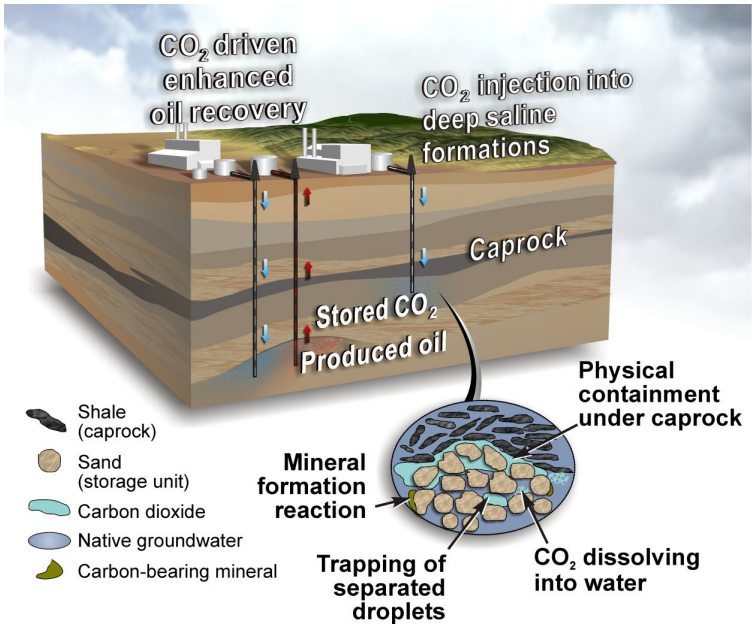

Use atomistic simulation to elucidate crack formation and propagation

- **Approach**:
  - Use atomistic simulation (e.g. molecular dynamics) to study crack formation at solid-fluid interface and how this process, and propagation is influenced by fluid and surface chemistry.
  - Upscale atomic quantities to continuum fields and use continuum theories of crack propagation to interpret simulation results.

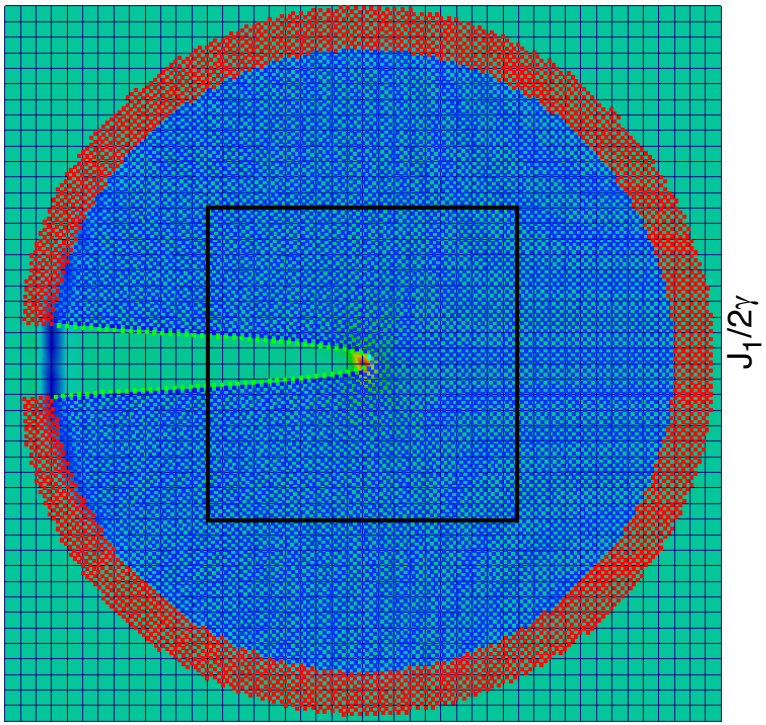

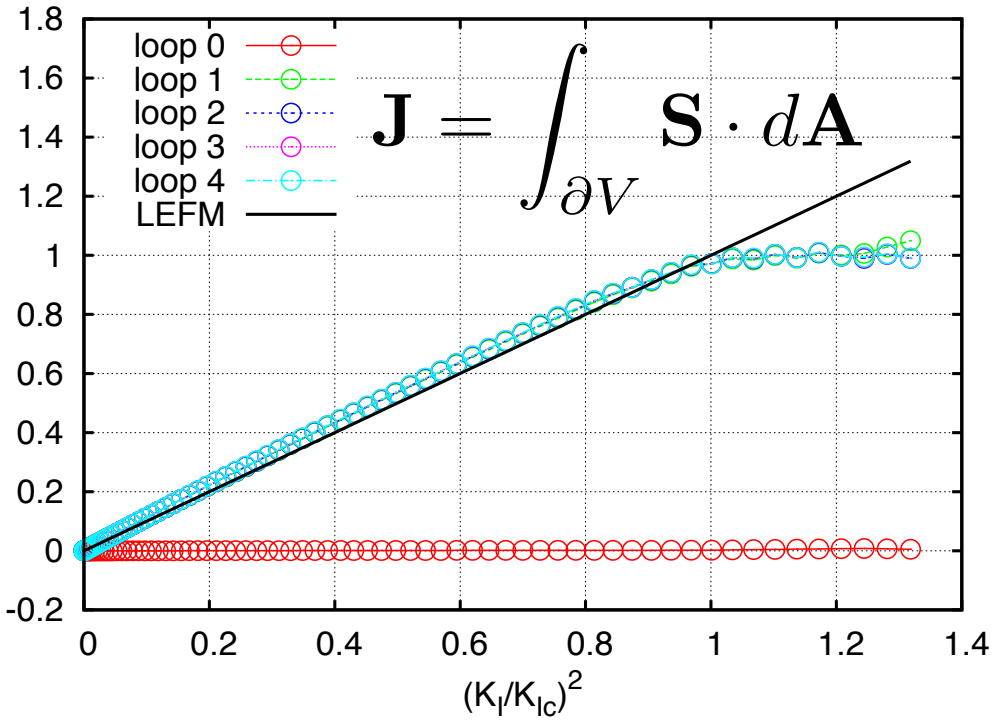

Upscaling accomplished using method by Hardy

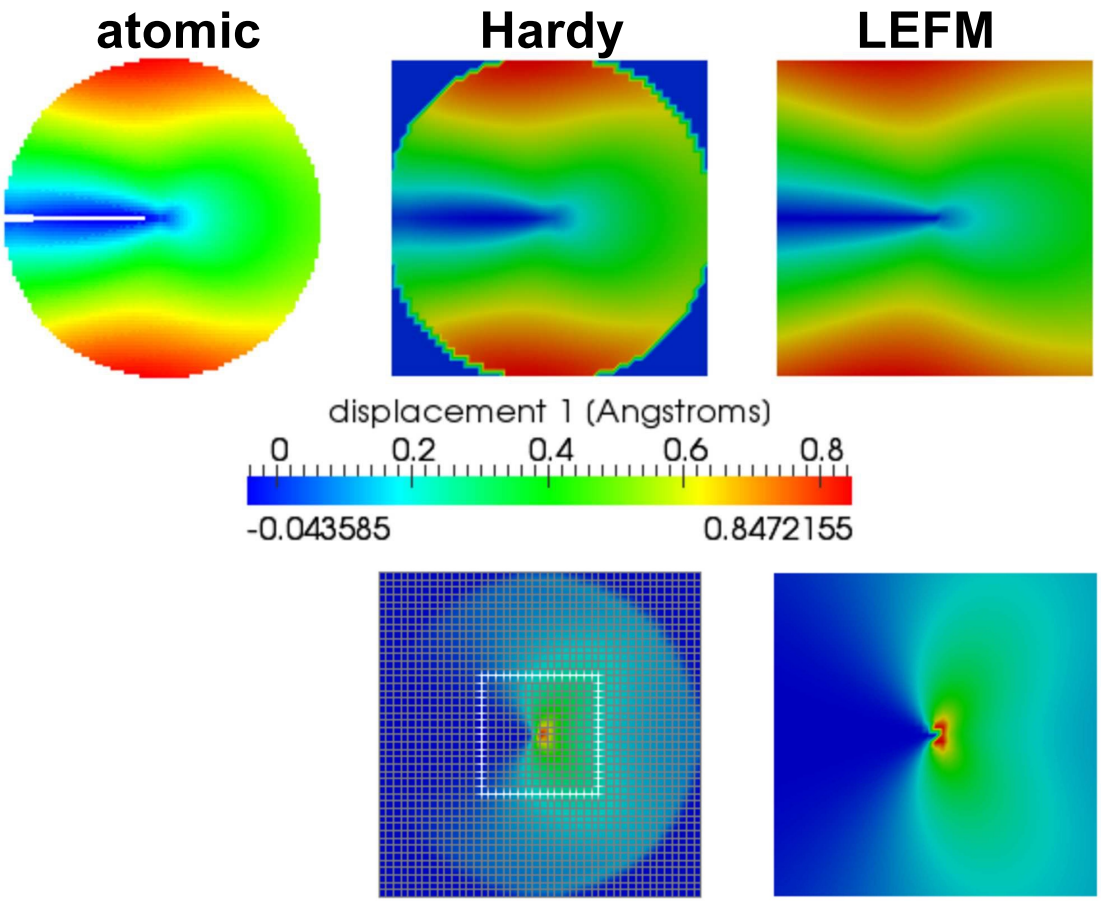

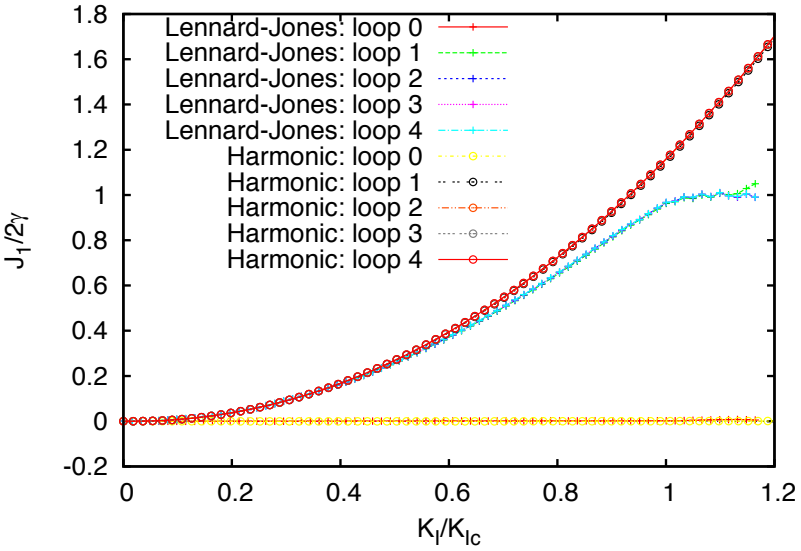

Upscaling of Hardy method and use in J-integral calculation exhibits path-independence and confirms expected fracture toughness

We've adapted this method to quasi-static, finite temperature scenarios

Simulations of SiO_2 with ReaxFF (force field)

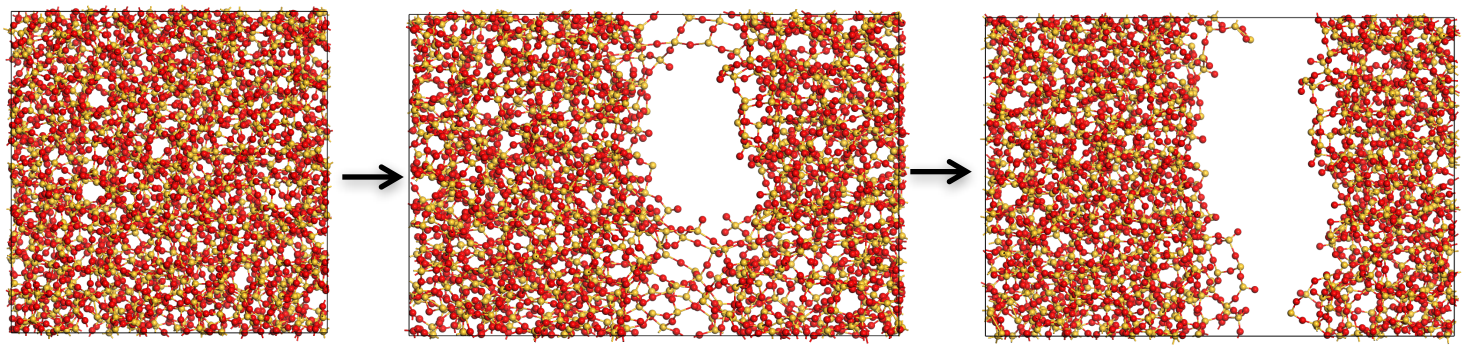

ε=0
Dense Silica

ε~0.35
Void nucleation and fracture initiation

ε~0.4
Fracture

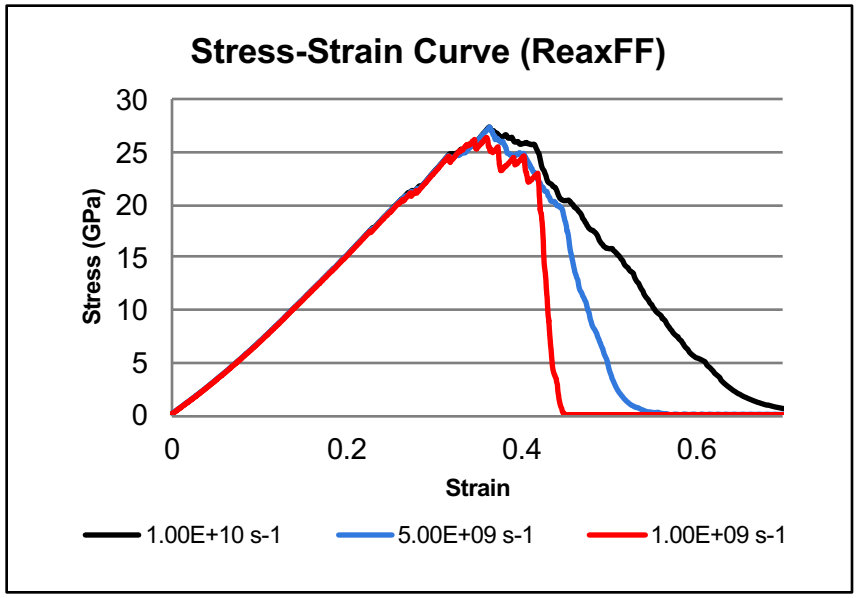

Silica is present in sandstone and shales.

Simulations show "rate-dependent" behavior during decohesion.

In progress: parameterization of ReaxFF potential for clay materials (KCl structure).

Progress on current effort for chemical reactivity

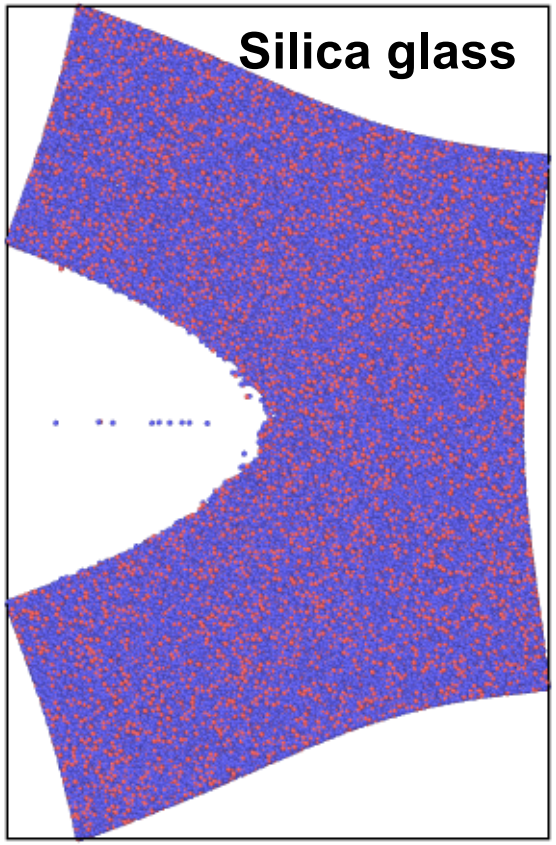

Wall regulates pressure in fluid

Fluid infiltration

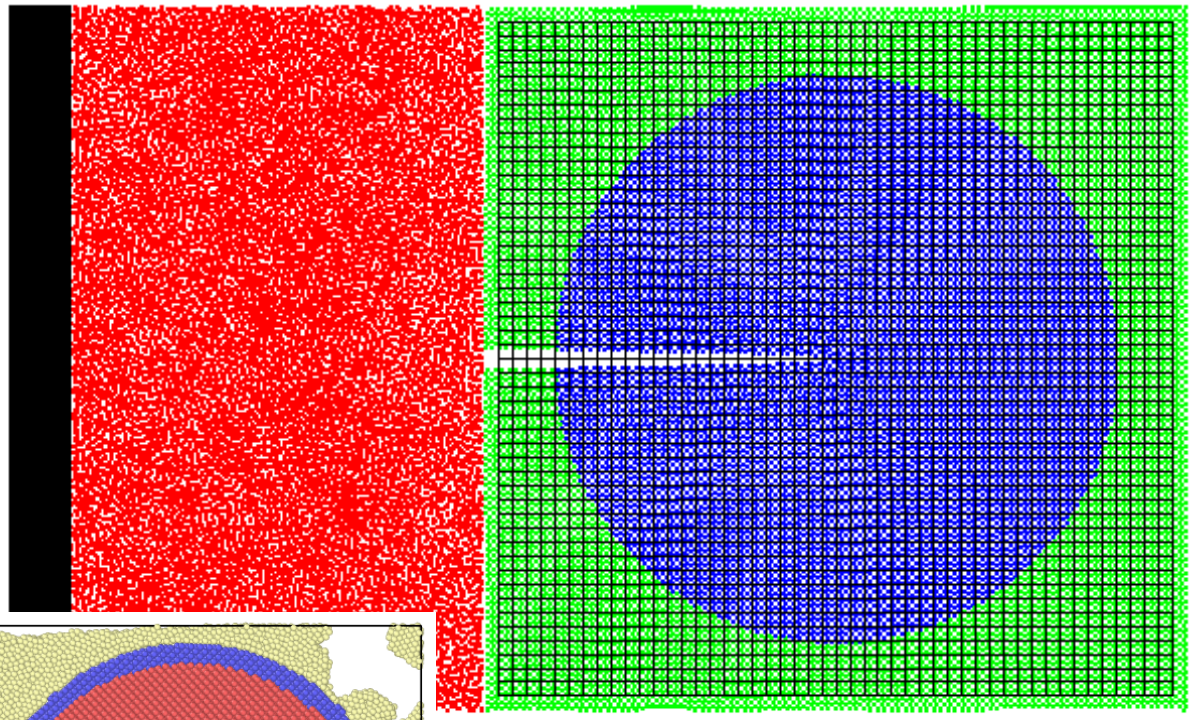

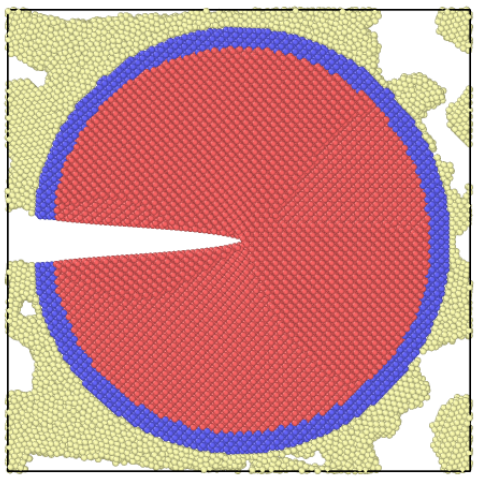

Green atoms provide far-field loading of the crack and allow access of the pressurized fluid

Calibration of strength and failure models to model ductile failure under shear-dominated states

Plate puncture problem: determine minimum puncture velocity and mode of puncture

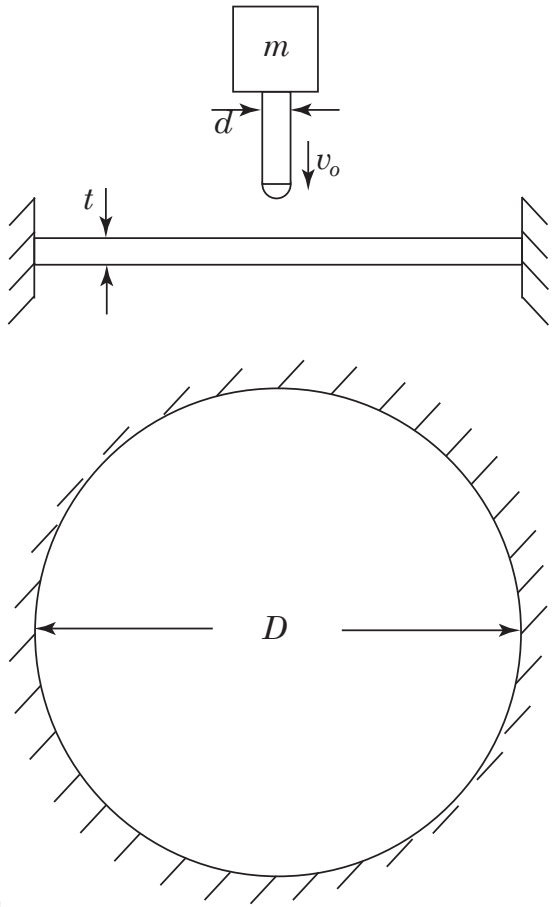

m = 306 lb
D = 6.75 in
d = t = 0.5 in
Al 7075-T651

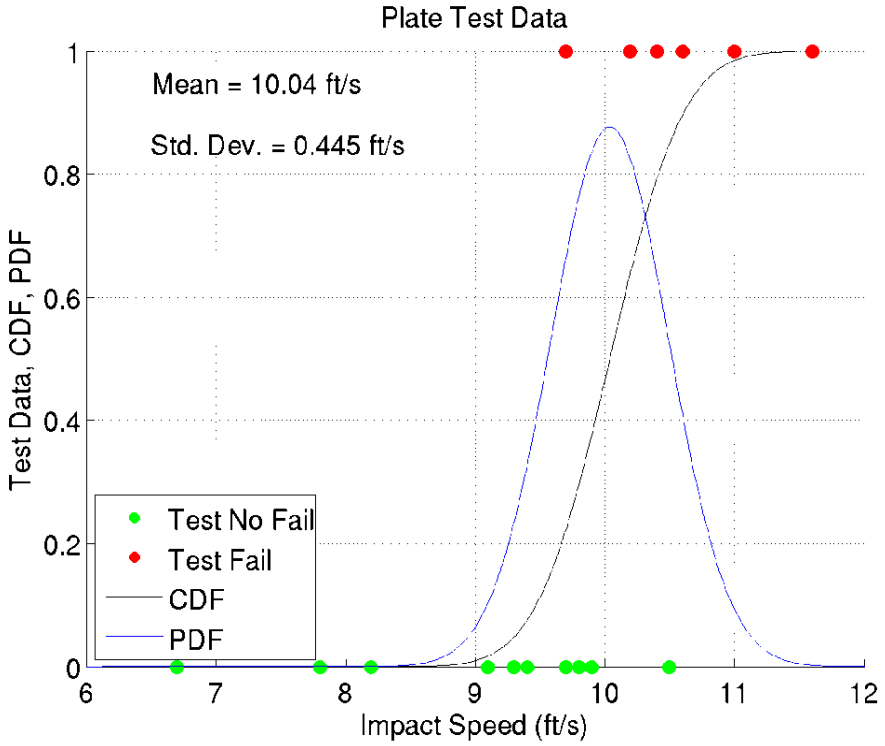

Numerical simulations

Sandia National Laboratories

FEM Model:

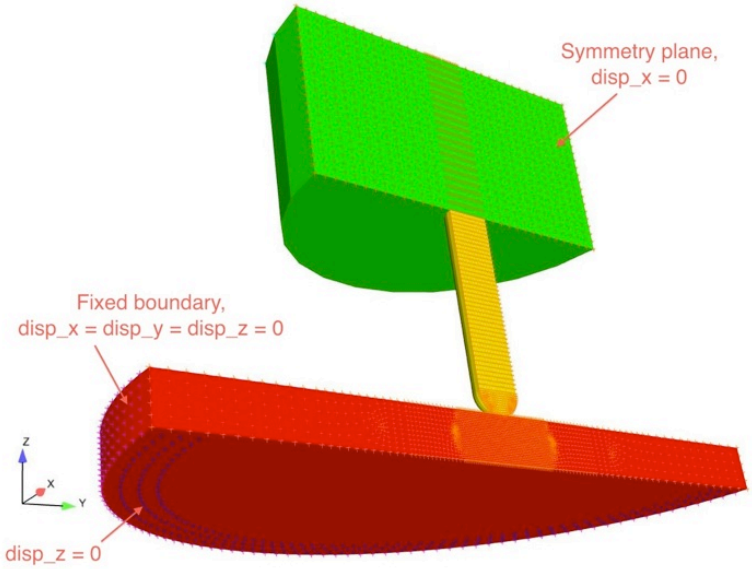

- 3-D model with 8-node hexahedral elements
- One plane of symmetry
- Explicit dynamics formulation
- Adiabatic – significant heat generation during plastic deformation

Plate Material Model:

$$\sigma_e = \left[A + B\left(\varepsilon_e^p\right)^n\right]\left[1 + C\ln\left(\frac{\dot{\varepsilon}_e^p}{\dot{\varepsilon}_{eo}^p}\right)\right]\left[1 - \hat{T}^m\right]$$

$$\hat{T} = \frac{T - T_r}{T_m - T_r}$$

$$\varepsilon_{ef}^p = \left[d_1 + d_2 e^{d_3\eta}\right]\left[1 + d_4\ln\left(\frac{\dot{\varepsilon}_e^p}{\dot{\varepsilon}_{eo}^p}\right)\right]\left[1 + d_5\hat{T}\right] \qquad \eta = \frac{\sigma_m}{\sigma_e}$$

$$\Delta T = \frac{\beta W^p}{\rho C_p}$$

- J_2 elastic-plastic with isotropic hardening
- Johnson-Cook strength model
- Johnson-Cook ductile failure model
- Calibration through a series of material tests

Material testing for model calibration: rate and temperature-dependent tension

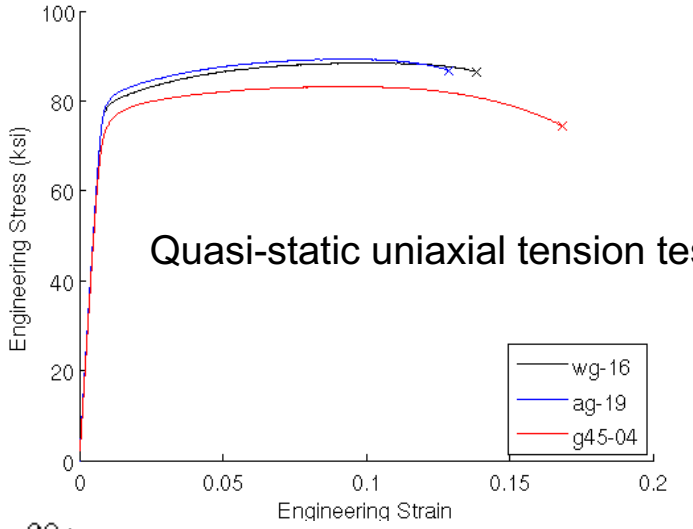

Quasi-static uniaxial tension tests

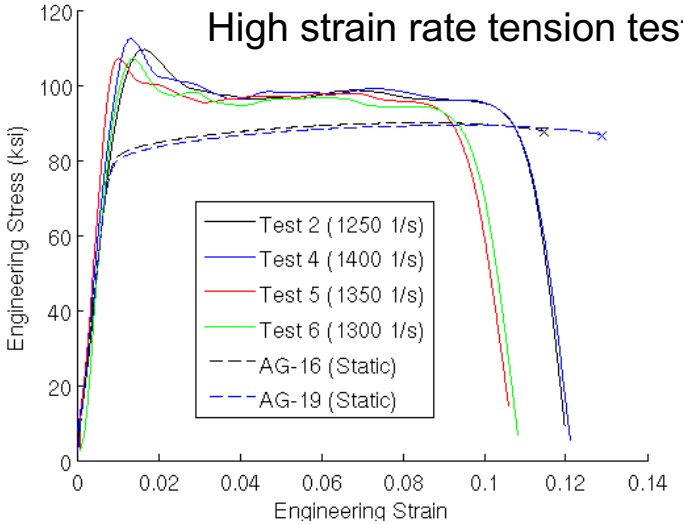

High strain rate tension tests

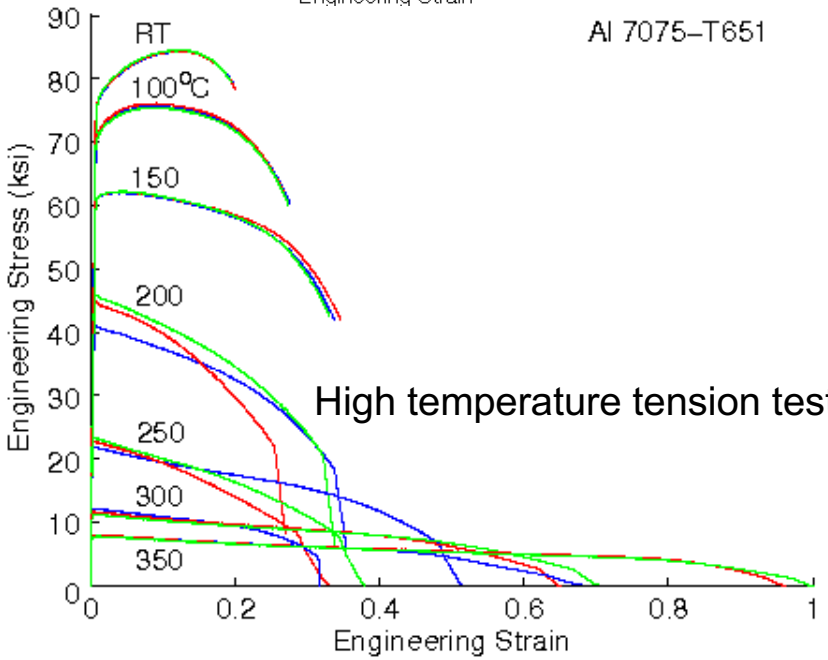

High temperature tension tests

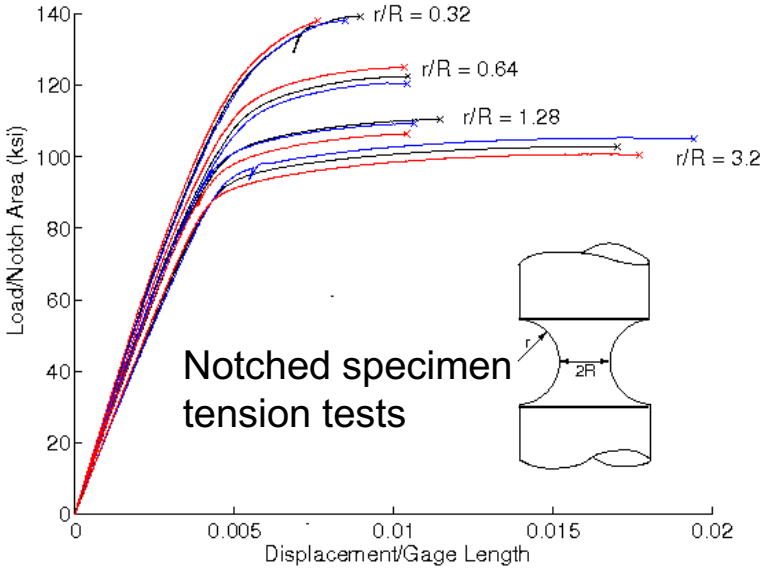

Notched specimen tension tests

FEM results are consistent with experiments with respect to threshold velocity and mode of failure

Sandia National Laboratories

Analysis Results:
- Threshold speed: [10,10.5] ft/s
- Mode of failure: Plugging

1 ms

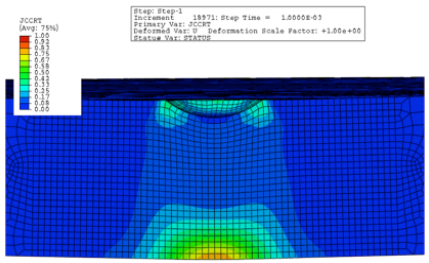

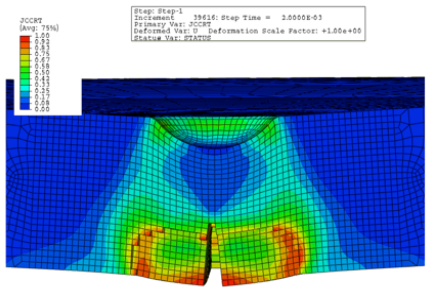

2 ms

3 ms

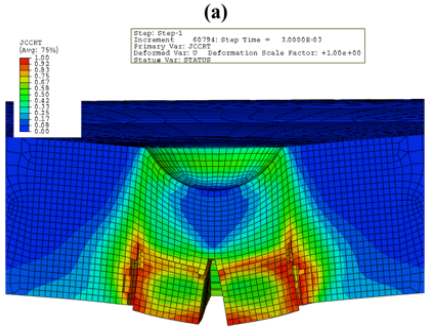

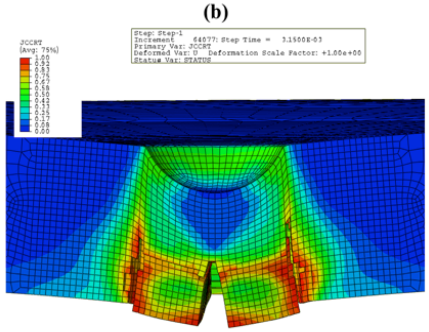

3.15 ms

3.2 ms

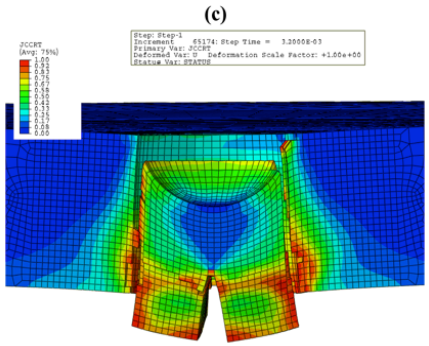

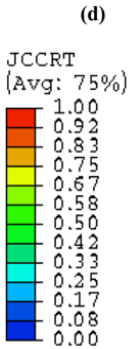

Comments:
- 3-D FEM model with 25 hexahedral elements through the thickness
- Johnson-Cook model provides a first order approximation of material behavior and failure for the aluminum alloys considered
- Analysis results are in reasonable agreement with experimental observations.

Cohesive zone-based fracture modeling of polymer/solid interfaces

- The performance and the reliability of many Sandia components depend on the integrity of interfaces between dissimilar materials
- **Goal**: Develop a finite element-based simulation capability to predict how variations in processing, environment, geometry, and loading affect the integrity of polymer/solid interfaces

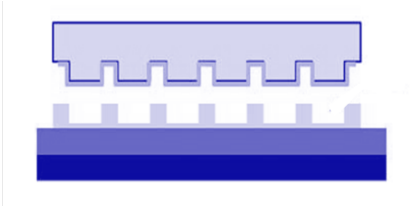

Nanoimprint lithography

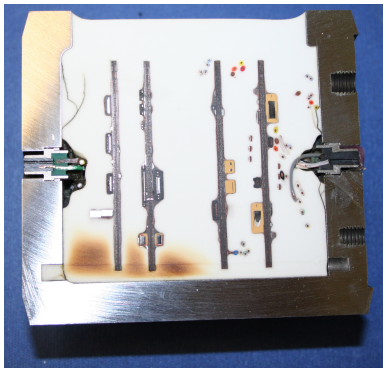

Fuze canister

Adhesively bonded stainless steel rupture disk

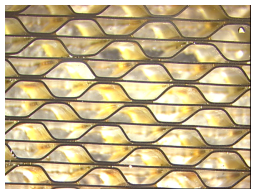

Aluminum Honeycomb

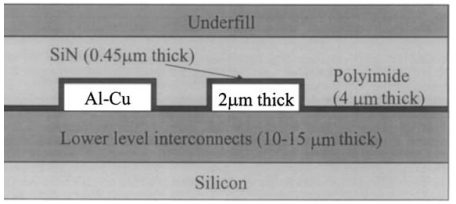

Thin films in microelectronics

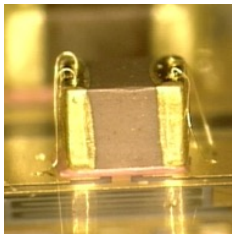

Adhesively bonded capacitors

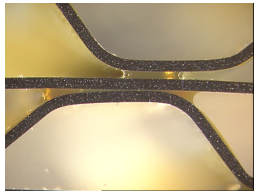

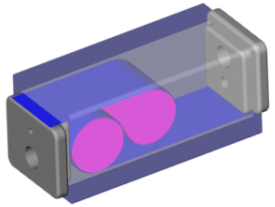

Bonded end caps in a switch

Interfacial toughness depends on mode mixity Ψ

- Mode mixity $\Psi_{r=l}$ is a measure of shear-to-opening deformation at the crack tip ($\Psi_{r=l}=0$ is pure opening)
- Interfacial cracks are subjected to a mixed mode loading because of material and geometric asymmetries

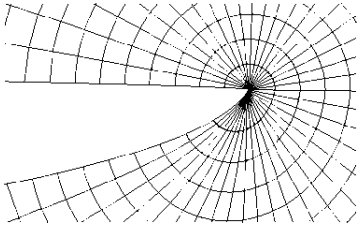

$$\Psi_{r=l_o} = \tan^{-1}\left(\sigma_{xy} / \sigma_{yy}\right)$$

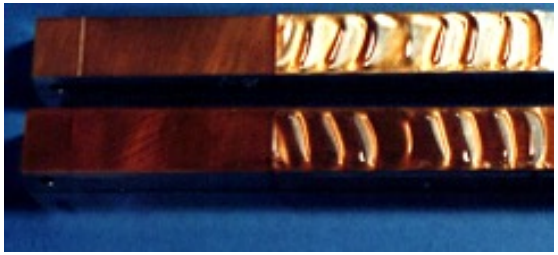

ADHERENDS SAME THICKNESS

$G_c = 140$ J/m^2

$\Psi_{l=10\ m} = 8^o$

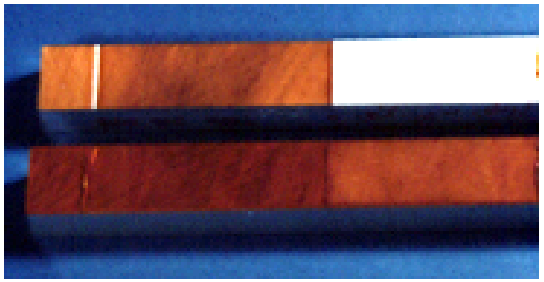

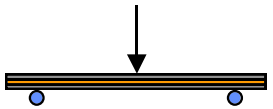

ADHERENDS SAME THICKNESS

$G_c = 2000$ J/m^2

$\Psi_{l=10\ m} = -83^o$

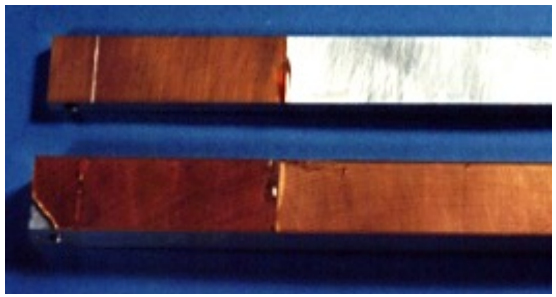

TOP ADHEREND HALF AS THICK

$G_c = 60$ J/m^2

$\Psi_{l=10\ m} = -8^o$

Developed a mode mixity-dependent cohesive zone model

CZM defines interfacial separation

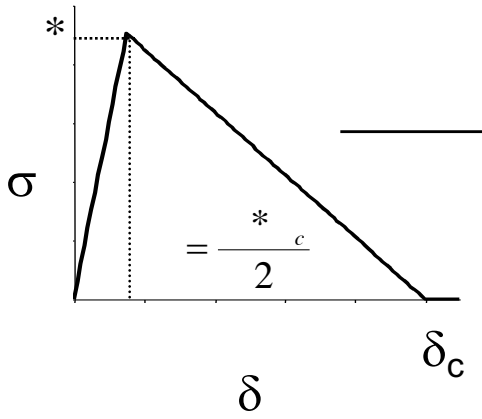

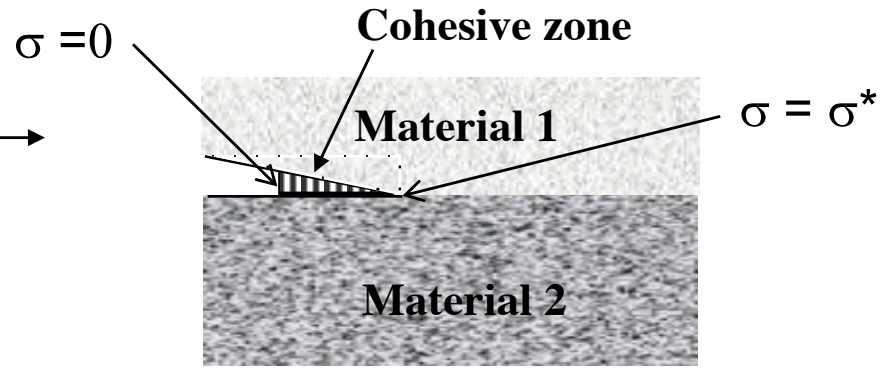

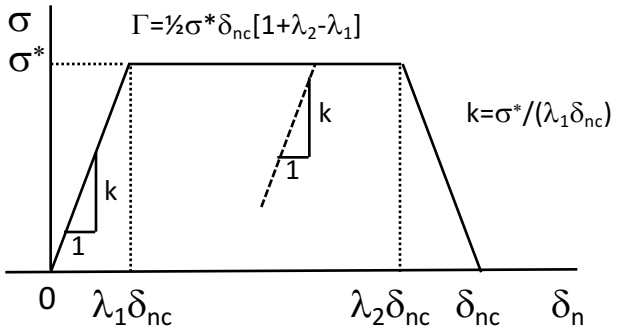

- Mode I dissipation depends only on normal separation

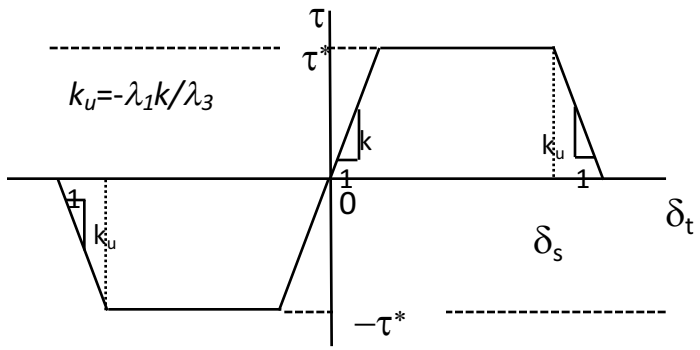

- Mode II dissipation by shear yielding along intact interface in front of CZ

CZM generates a Ψ–dependent toughness (Reedy and Emery, IJSS 2014)

CZM predictions match published data

- Swadener and Liechti, measured the interfacial toughness of a glass/epoxy interface (JAM, 1998)
  - E = 2 GPa, h=0.25 mm, and Γ=1.5 J/m^2
- Calculated effective toughness Γ_e in good agreement with data
  - displays similar asymmetric response
- Shape of calculated Γ_e/Γ *vs.* ψ_a relationship is not predefined

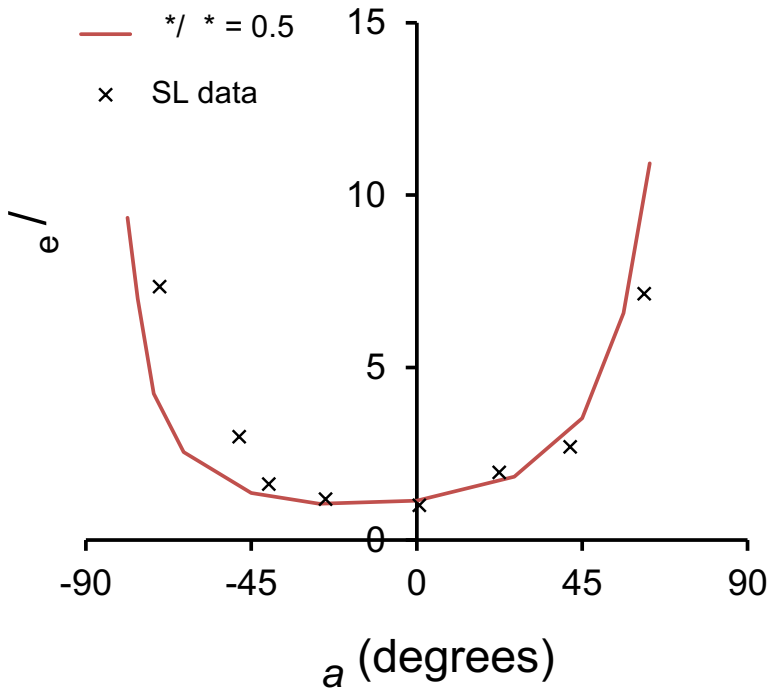

Capability enables predictions of life cycle history

- Implemented in SNL's Sierra/Solid Mechanics finite element code
- Enables predictions on how processing/life cycle history affects integrity of polymer/solid bonds in Sandia components
- Have begun to apply our new techniques to SNL problems

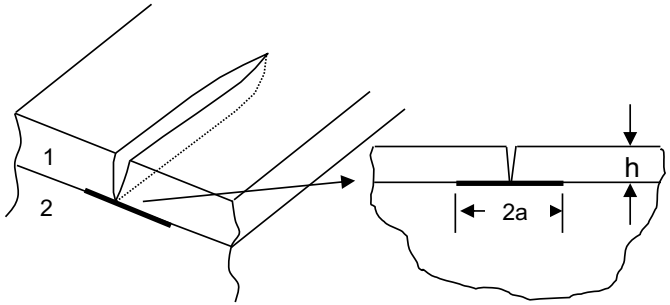

Interfacial cracking (delamination) from the root of a channel crack in a thin film.

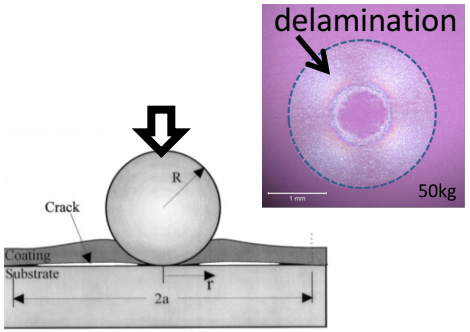

Interfacial cracking generated by indentation of a thin film.

Publications:

1. Reedy, E.D., Jr. and Emery, J.M., A Simple Cohesive Zone Model that Generates a Mode-mixity Dependent Toughness, International Journal of Solids and Structures (2014) p3727.
2. Reedy, E.D., Jr., Cohesive Zone Finite Element Analysis of Crack Initiation from a Butt Joint's Interface Corner. International Journal of Solids and Structures (2014) p4336.

Sandia's Fracture Challenges – predicting crack initiation and propagation across the mechanics community

- SFC1 and SFC 2 are computational challenges for predicting failure open to internal/external competitors
- 1st Challenge: Ductile tearing of 15-5 PH
  - Modified C(T) specimen with 3 holes in front of primary notch
  - 10 specimens tested at SNL, 3 at UT-Austin
  - Loading rate of 0.0127 mm/s
  - 13 teams competing from SNL, academia, industry
  - **B.L. Boyce *et al*, *Int. J. Fract*. (2014)**
- 2nd Challenge: Variable rate, mixed-mode crack initiation and propagation in Ti-6Al-4V sheet
  - Included two data sets for material model calibration, geometry information, and test procedures
  - Success = correct crack path and accurate load-displacement curves for two rates: 25.4 mm/s and 0.0254 mm/s pin loading rates
  - **B.L. Boyce *et al*, *Int. J. Fract*. (2016)**

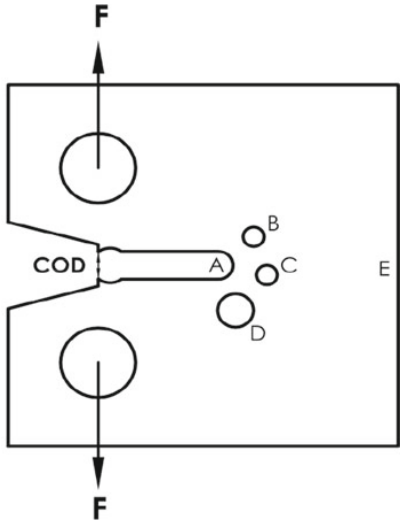

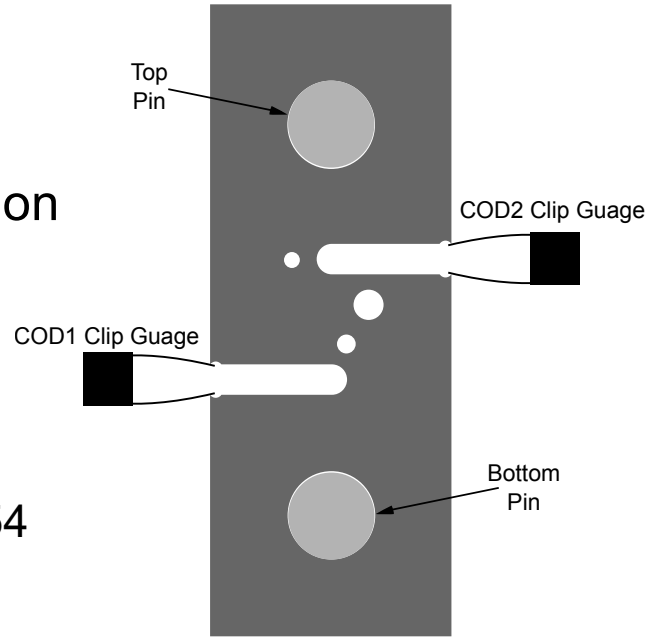

1st Fracture Challenge: Dimensional accuracy is crucial

- Of 13 specimens, 3 were found to not meet dimensional accuracy (±50.8 mm) regarding distances between holes
- 10 specimens predicted A-D-C-E path, 3 for A-C-E

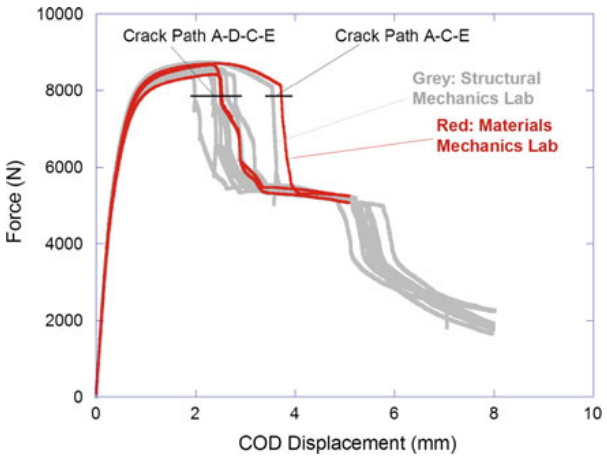

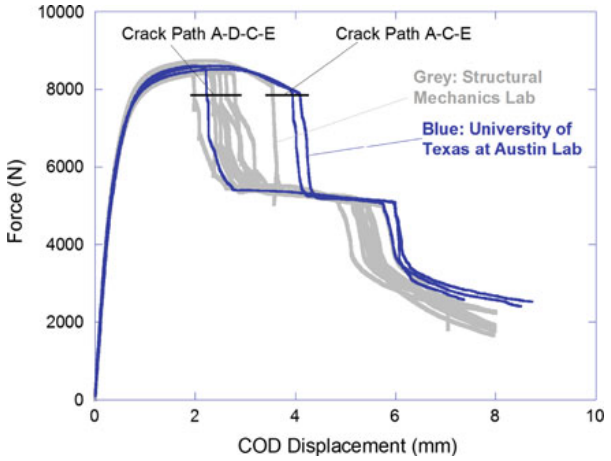

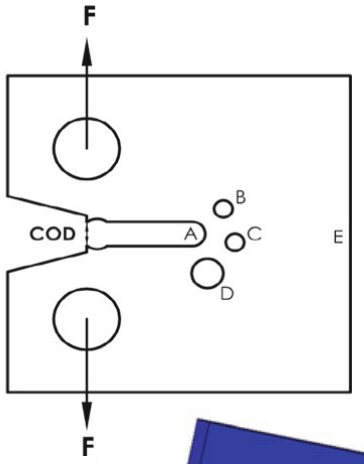

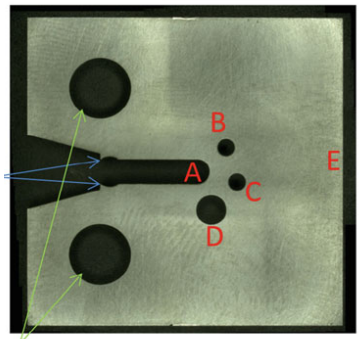

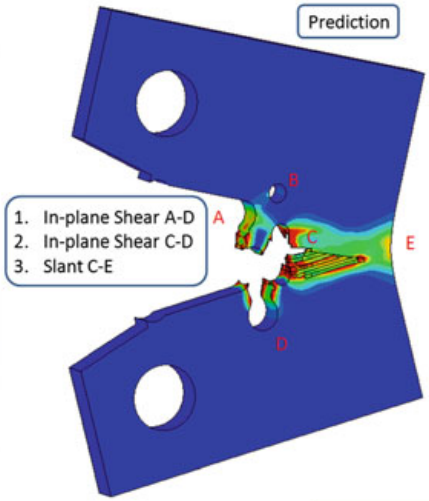

- Predictions: 4 teams predicted A-D-C-E, 9 for A-C-E
- Closest predictions by:
  - Xue (Schlumberger) – Damage plasticity model with stress-based fracture envelope
  - Gross, Ghahremaninezhad and Ravi-Chandar (UT-Austin) – Power-law plasticity + Johnson-Cook failure model
  - Pack, Luo, Wierzbicki (MIT) – 3-parameter Modified Mohr-Coulomb model

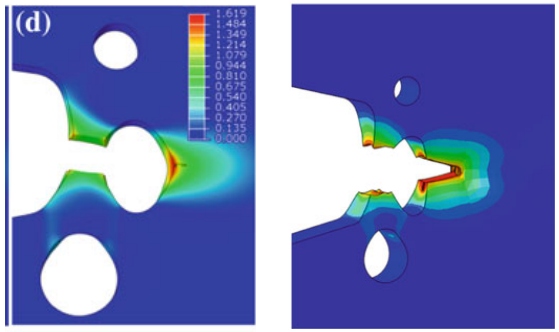

1st Fracture Challenge: Lessons learned

- Availability of calibration data is important
- Geometric uncertainties were shown to have a huge impact on crack path predictions
- Mesh convergent methods remain an open issue
- Effects of microstructure may be important but were not included by any of the teams
- Improved physical descriptions of fracture are necessary to reduce dependence on empirical material testing
- A trade-off is necessary between physical realism and computational efficiency

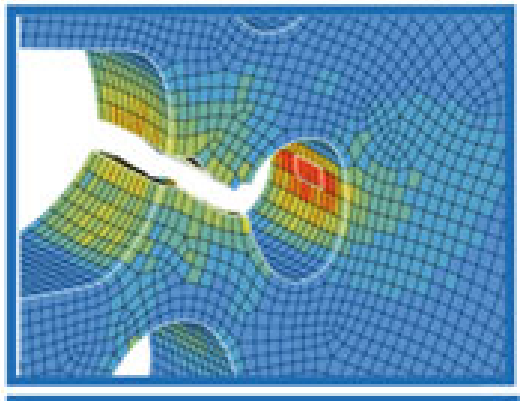

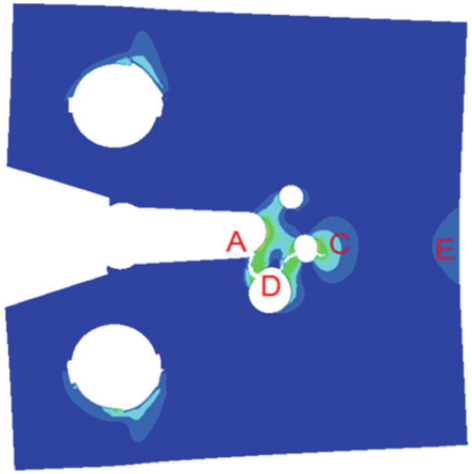

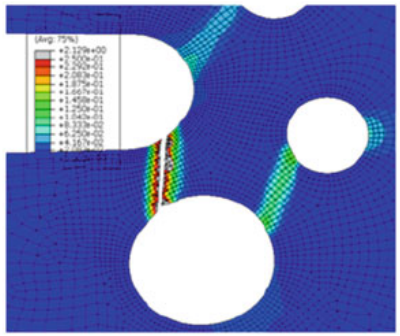

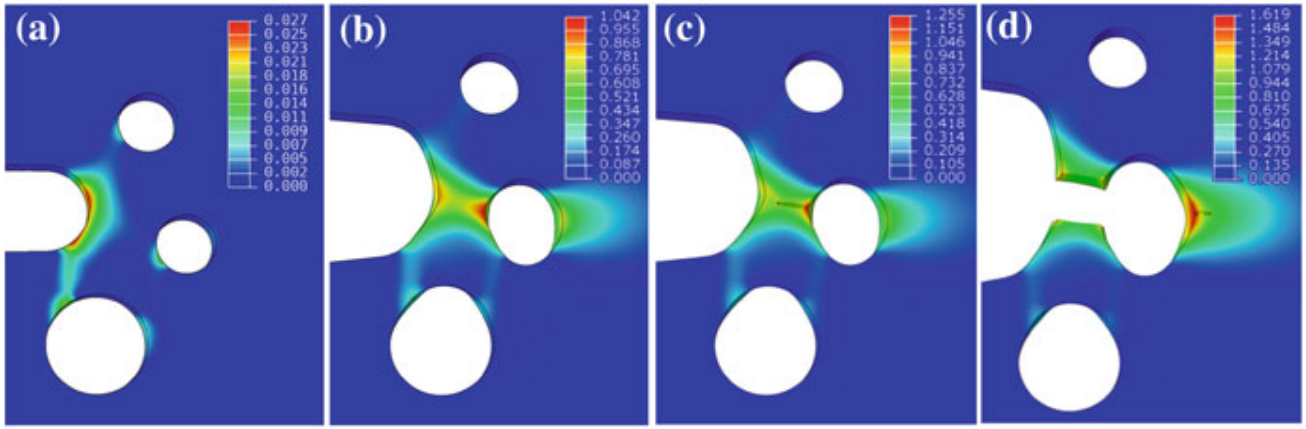

2nd Fracture Challenge: Anisotropy and rate effects

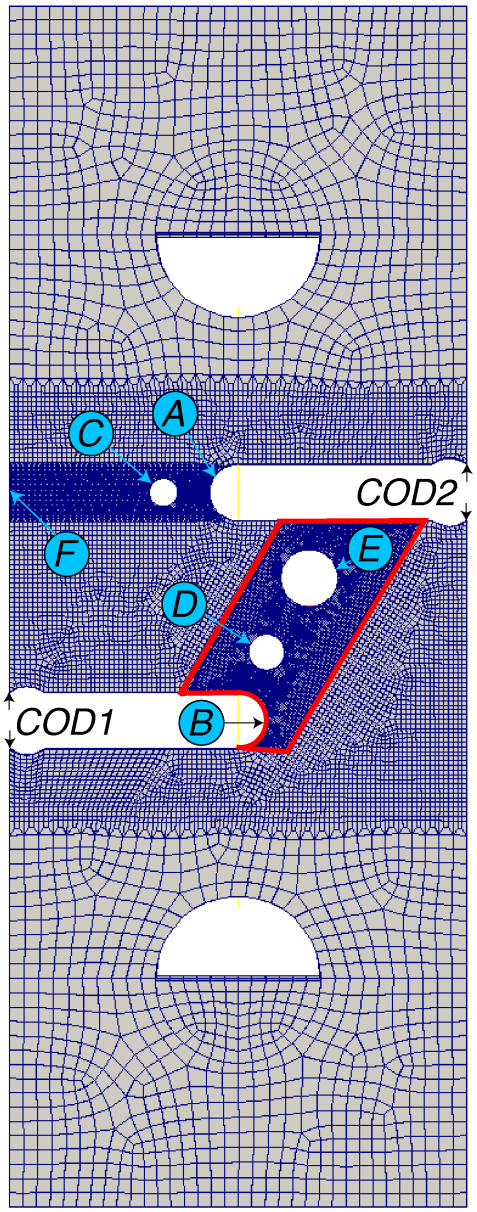

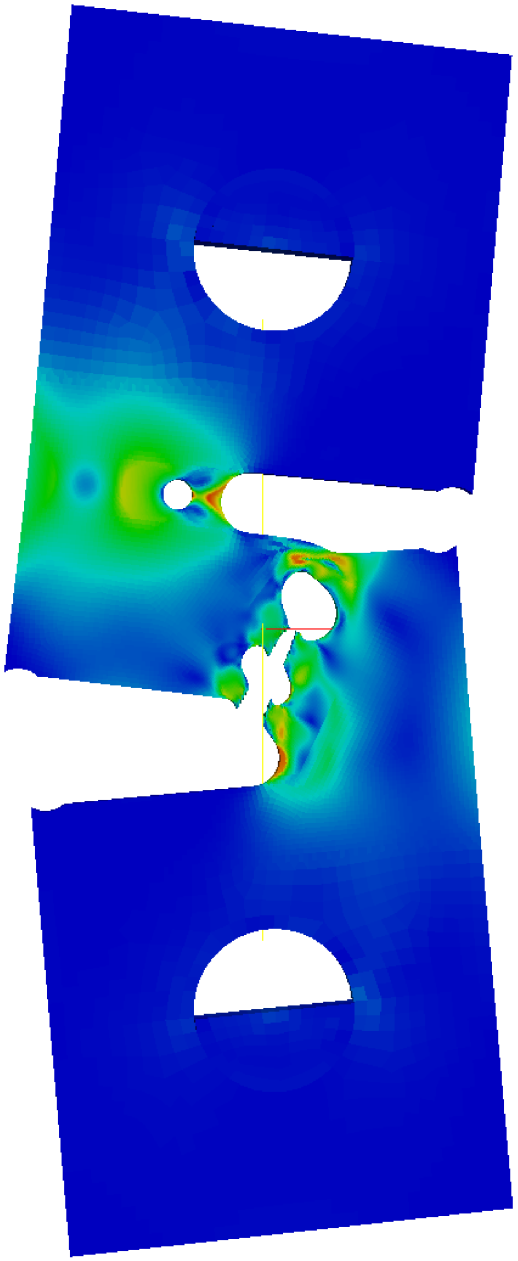

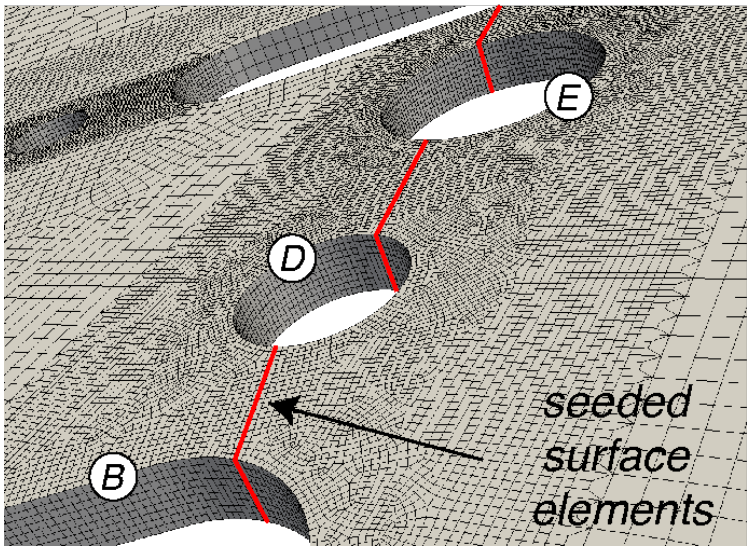

- Ti-6Al-4V plate
- Anisotropy
- Mixed-mode loading
- Slow/fast rates of loading
- Thermomechanical coupling
- Dynamics (unstable propagation)
- Employed surface elements
- Multiple damage models
- Implicit solution
- *Sierra SolidMechanics*

Data provided for modeling teams

- Detailed engineering drawings with tolerances
- Dimensional measurements of all test coupons
- Grip details
- Heat treatment details, with hardness values
- Extensive tensile data (2 rates, 2 orientations, 5 tests each)
- Extensive shear deformation & failure data (non-standard)
- Fixture compliance measurements
- Deformed shape
- Fractography

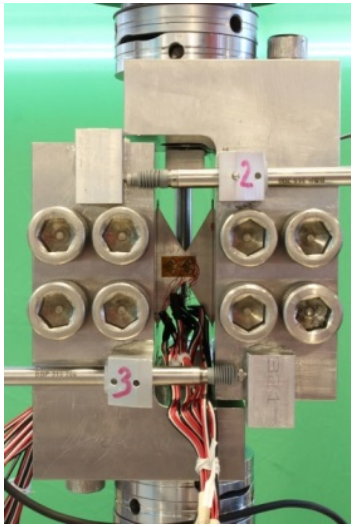

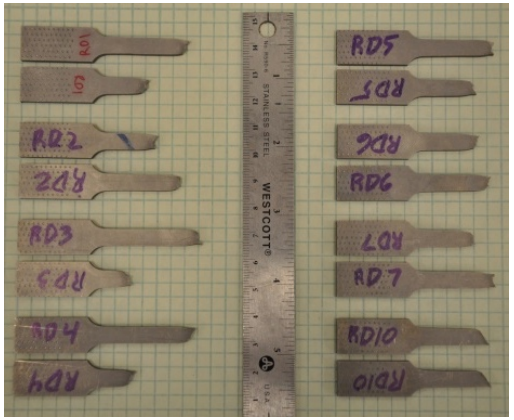

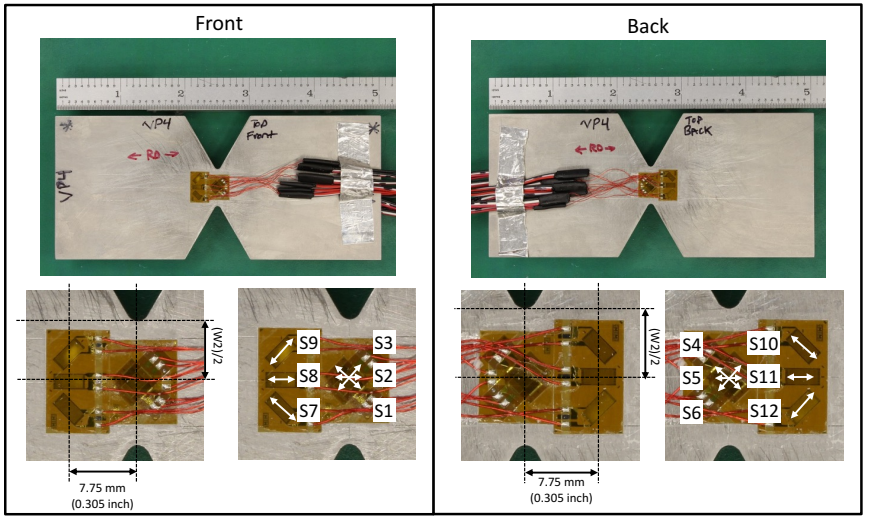

Sandia team

Sandia National Laboratories

- Jay Foulk, Kyle Karlson, Arthur Brown, Mike Veilleux, Wei-Yang Lu, Tracy Vogler, Jake Ostien, Bill Scherzinger, Alejandro Mota, John Emery, Lauren Beghini, Kendall Pierson
- Sandia codes and tools used for analysis: *SIERRA Solid Mechanics (SM)*
- Time scales for characterization and testing require *implicit* analysis, *implicit dynamics* required for unstable crack growth
- Low thermal conductivity demands *thermomechanical* coupling
- Provided experimental data and the literature advocate
  - *Rate* and *temperature* dependence
  - *Anisotropy* in yield stress and hardening
  - *Void evolution* (multi-axial nucleation, growth, coalescence)
- We resolve fields in space/time with *Q1P0, hex 8 elements* on the order of 0.175mm
- We seek to *regularize* the solution through multiple technologies
  - Nonlocal method retains multiphysics. Refinement needed.
  - Localization elements enable *efficient* and *stable* solutions

Material model

- From the start, we knew we needed a constitutive model with the following capabilities:
  - Strain-rate dependence
  - Temperature dependence
  - Damage/failure in tension and in shear
  - Anisotropic yield and hardening behavior

SIERRA SM Elasto Viscoplastic (EV) Model

$$\dot{\eta} = \eta \dot{\epsilon}_p N_1 \left[\frac{4}{27} - \frac{J_3^2}{J_2^3} \right]$$

$$\dot{\phi} = \sqrt{\frac{3}{2}} \dot{\epsilon}_p \frac{1-(1-\phi)^{m+1}}{(1-\phi)^m} \sinh \left[\frac{2(2m-1)}{2m+1} \frac{\langle \frac{I_1}{3} \rangle}{\sqrt{3J_2}} \right]$$

$$\sigma_y = \left(Y(\theta) \left\{ 1 + \sinh^{-1} \left[\left(\frac{\dot{\epsilon}_p}{f(\theta)} \right)^{1/n(\theta)} \right] \right\} + \frac{H(\theta)}{R_d(\theta)} \left(1 - e^{-R_d(\theta)\epsilon_p} \right) \right) (1-\phi)$$

Boyce and Kramer

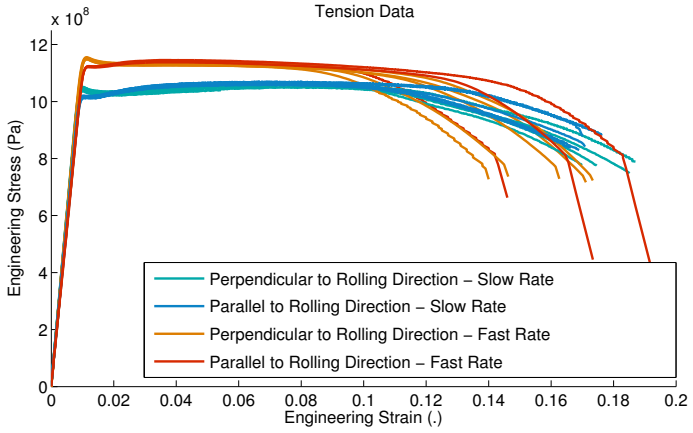

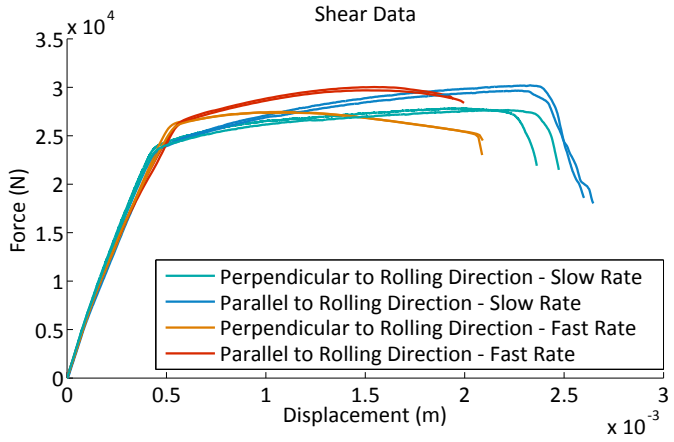

$Y^t = 493$ MPa $\quad H = 3084$ MPa $\quad R_d = 13 \quad \beta = 0.8$
$f = 1 \times 10^{-6} \quad n = 26 \quad m = 6 \quad N_1 = 54$
$\phi_0 = 1 \times 10^{-4} \quad \phi_0^\eta = 2 \times 10^{-5} \quad \eta_0 = 5 \quad \phi_{coal} = 0.15$

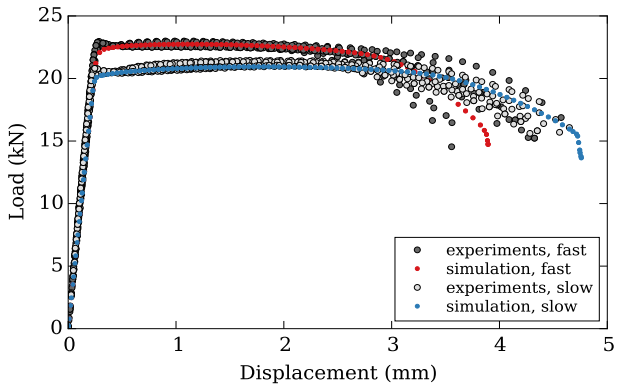

Including anisotropy

- Calibrated a Hill, anisotropic yield surface to the shear and tensile data
- Anisotropic yield predicted SFC would localize in the lower notch
- Lower notch experiences shear loading and rate/temperature effects are still important
- Vary isotropic material properties in regions with shear loading to mimic simulation results using the Hill, anisotropic yield surface

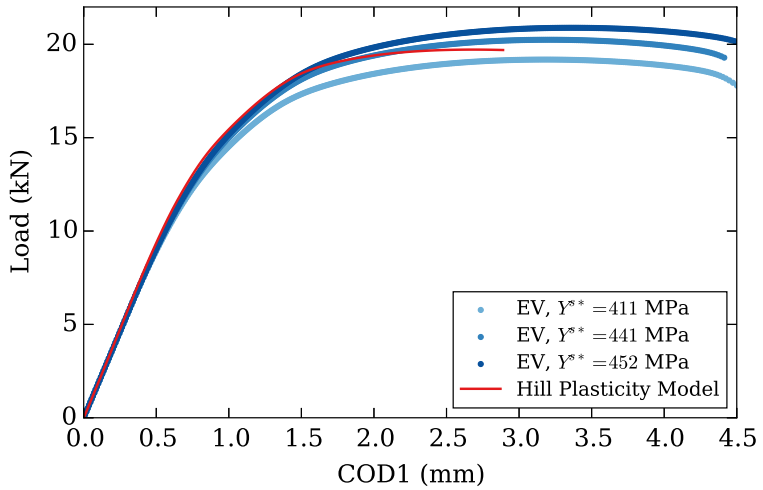

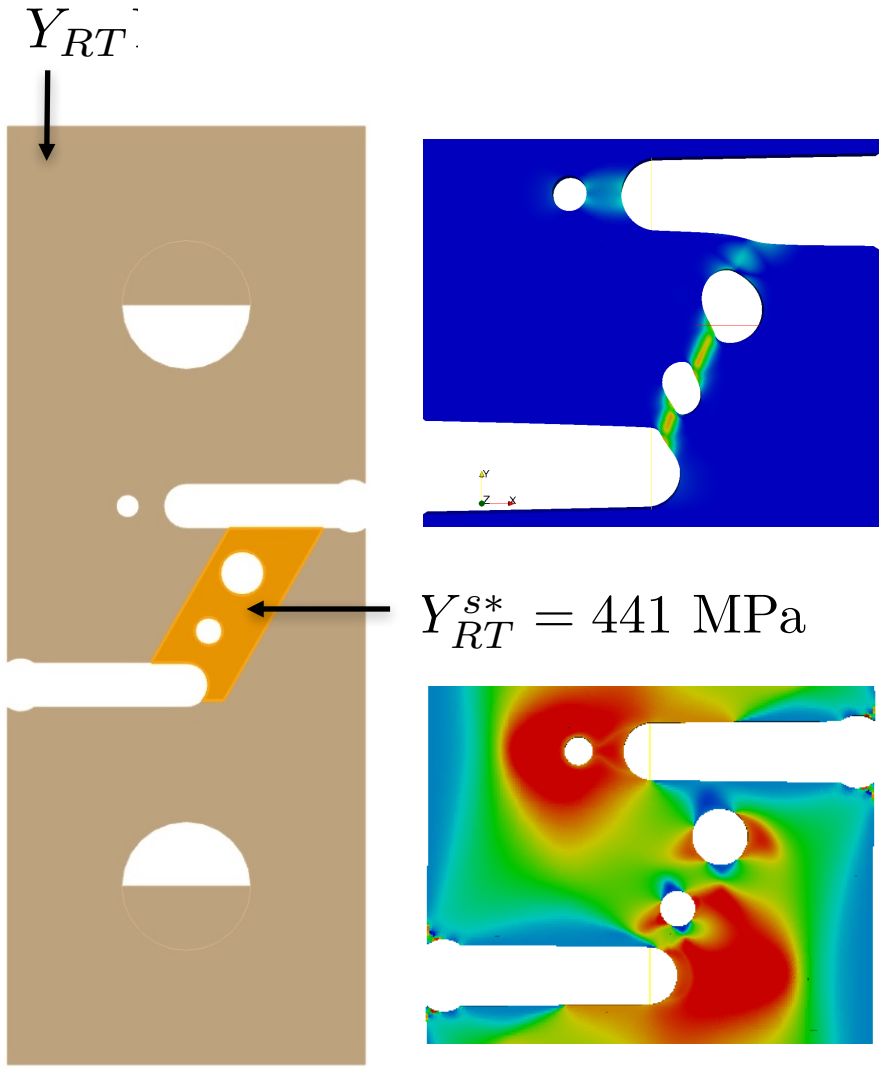

Prediction compared to experiment: SNL results

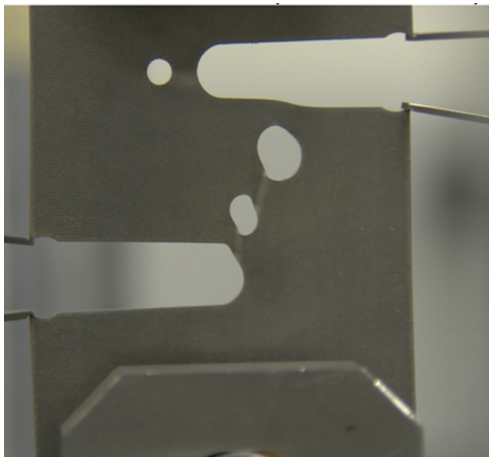

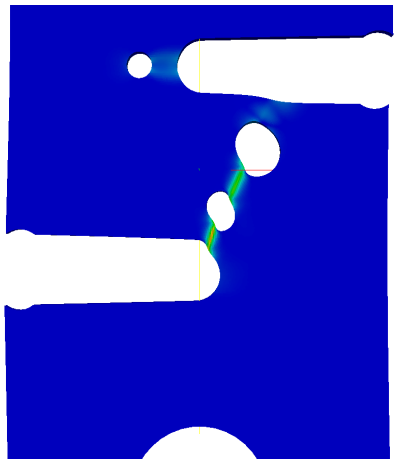

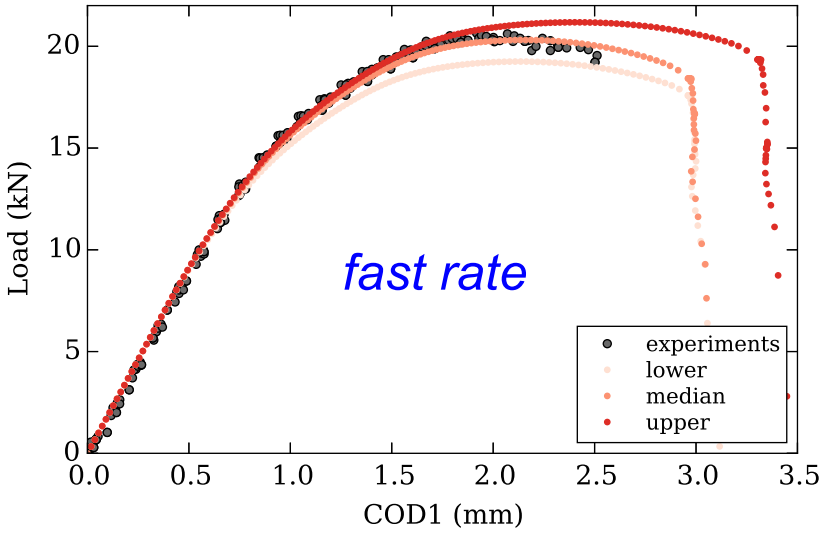

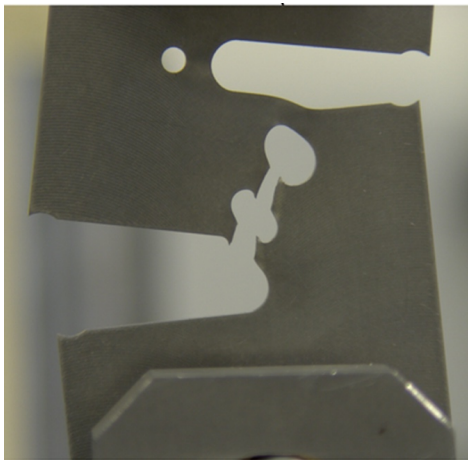

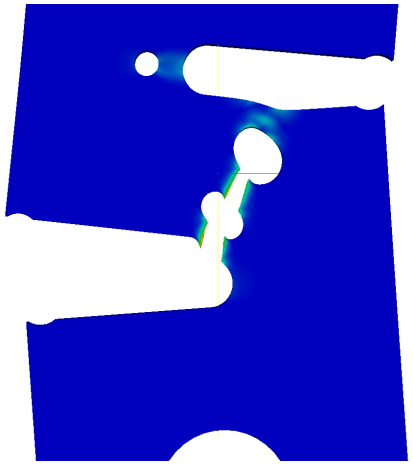

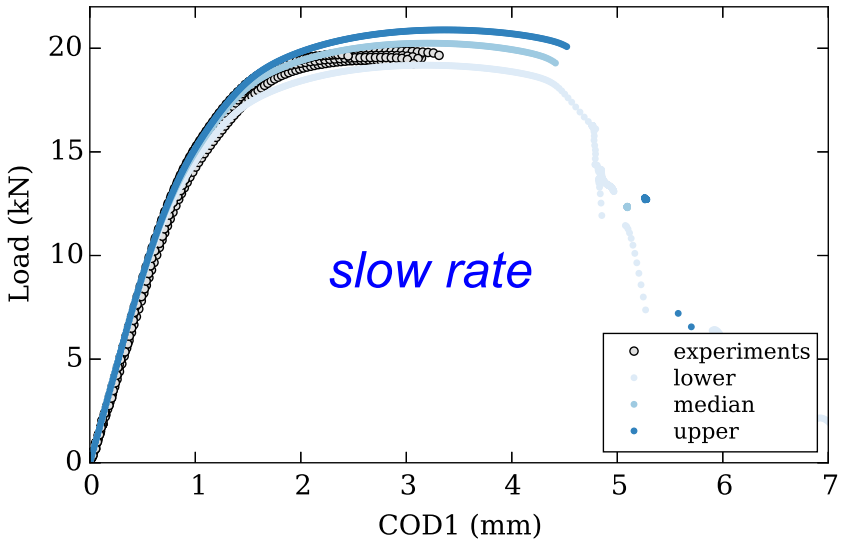

Prediction compared to experiment: all teams

- Most teams predicted the correct crack path
- Not a single team predicted the load-displacement curves within the experimental data for both rates

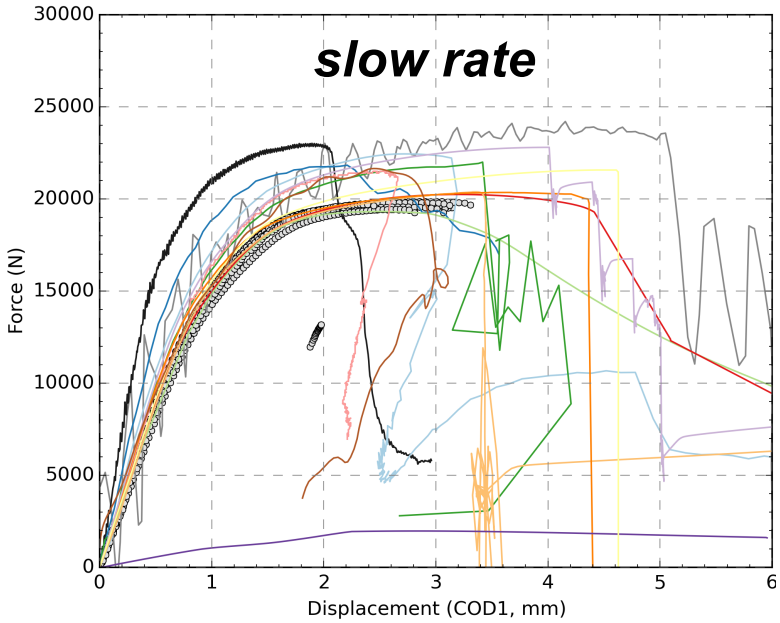

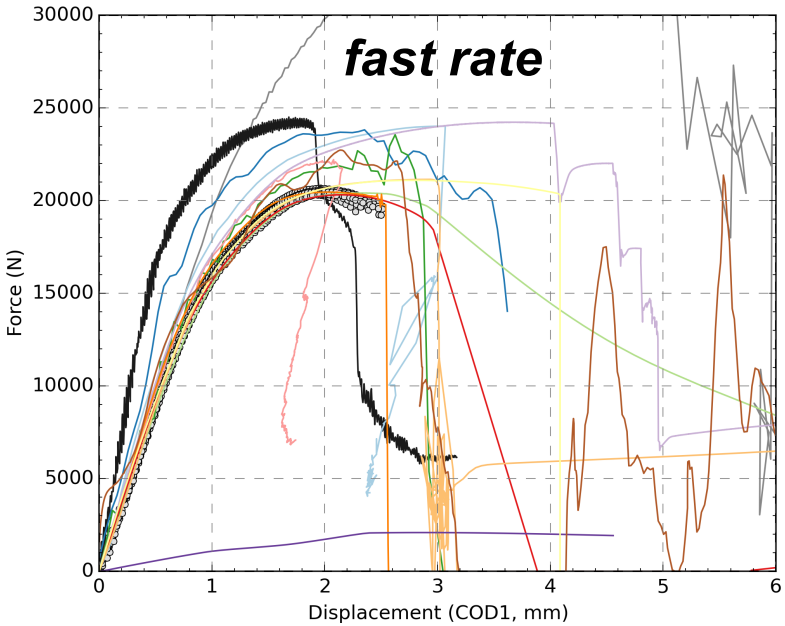

- No team rigorously accounted for material/geometric variability
- Almost all teams over-predicted the loads and displacement to failure

Lessons learned from 2nd fracture challenge

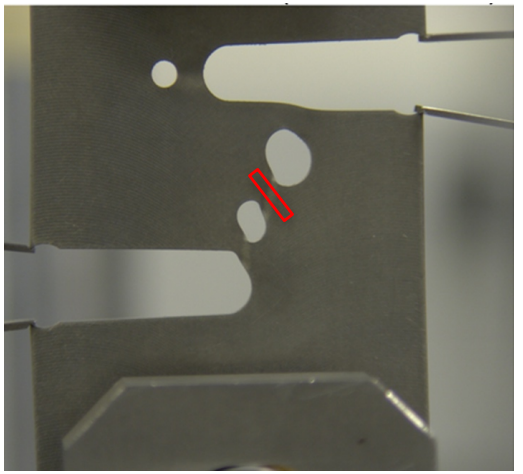

- Crack path dependent on inclusion of *anisotropic yield surface*
- *Thermomechanical modeling* with *rate* and *temperature dependence* required to capture necking behavior
- *Void nucleation* is the observed failure mechanism
- Too much flexibility may convolute different physics and lead to non-uniqueness
- Physics of interest must exist in the code to determine how/if these physics affect the solution.
- More test standards for material characterization needed
- Shear testing required; tension tests are not enough
- Conversion of plastic work to heat
- **Paths forward:**
  - Enhance code robustness to include failure/contact and thermo-mechanical coupling
  - Improve mesh independent failure methods: localization elements and non-local failure
  - Modeling and characterization should include: anisotropy, damage, dynamic strain aging and crystal plasticity

Final Thoughts

- Hopefully, I've given you a brief view on fracture mechanics R&D at SNL.
- Key themes:
  - Microstructure can play a large role, especially for aging and reaction processes
  - Considerations of microstructure, **anisotropy**, **stress triaxiality**, nucleation and rate effects can impact the fidelity of models and predictions, but level of fidelity needed should be evaluated.
  - Various modeling approaches all have value, and many provide essentially the same result.
- Examples of fracture in thin sheet materials:
  - Plate puncture problem: t/D ~ 0.074 → shear dominated failure
  - 1st Fracture challenge: a/W = 0.577, t/W = 0.095, $R_{B/C}$/W = 0.020, R_D/W = 0.046
  - 2nd Fracture challenge: a/W = 0.525, t/W = 0.061 $R_{A/B/E}$/W = 0.063, R_C/W = 0.031, R_D/W = 0.039
- Our interests in thin sheet metals and microstructure-based fracture modeling (http://www.sandia.gov/PPM/)